Structure and Metamorphism of the Elk City Area, North-Central Idaho

Joe D. Dragovich
Russell F. Burmester
Reed S. Lewis

Idaho Geological Survey
University of Idaho
Moscow, Idaho 83844-3014

Technical Report 09-1
ISBN 1-55756-516-2

Contents

Figures

Structure and Metamorphism of the Elk City Area, North-Central Idaho

Joe D. Dragovich[1 2]
Russell F. Burmester[3]
Reed S. Lewis[1]

ABSTRACT

Structural analysis of the Red River Hot Springs-Elk City area indicates it was affected by at least five deformational events (D1-D5). D1 produced a regionally extensive mica foliation (S1). S1 is axial planar to rarely observed recumbent isoclinal folds (F1) of bedding but generally is parallel to bedding in the metasedimentary units. D2 is characterized by shallowly northwest-plunging tight folds (F2) of S1 foliation. Some F2 folds contain a weakly developed axial planar foliation (S2) defined by muscovite and biotite. F2 folds range from upright to inclined or overturned to the southwest. Their axes parallel L2 lineations, which consist of crenulations, mineral (hornblende, biotite, sillimanite) lineations in metasedimentary rocks and amphibolites, and stretching lineations defined by augen in the augen gneiss of Red River and megacrysts in tectonized Cretaceous granodiorite; all are parallel. D3 refolded the F2 folds about northeast-trending axes; F3 open folds lack axial planar fabric. North-striking faults formed during D3, and some are mineralized. D4 is characterized by northeast-striking, high-angle normal faults that commonly show a small component of sinistral strike-slip movement. D5 is recorded by accumulations of unconsolidated sediments confined by reactivated north-striking faults in the Elk City area and farther west.

Constraints on the age and origin of these deformations suggest that most are Cretaceous or younger. D5 is probably Miocene, a northern expression of Basin and Range extension. Much of the D4 fault movement is probably Eocene because dikes of probable Eocene age invade the faults, some of those dikes are mylonitized, and the faults offset epizonal Eocene granite. S-C mylonites and biotite fish in sheared dikes near the Bargamin fault give a normal, down-to-the-northwest sense of displacement consistent with regional Eocene extension directions. D4 postdates peak metamorphism because mylonites associated with the faults contain retrogressive mineral assemblages. The age of D3 is probably best quantified by a 69 Ma $^{40}Ar/^{39}Ar$ date on secondary muscovite in a north-striking fault, but folding may be as young as 60 Ma metamorphism documented to the north. At least part of D2 is Cretaceous, as indicated by the parallelism of fabrics in metamorphic rocks and the megacrystic granodiorite whose $^{40}Ar/^{39}Ar$ hornblende cooling age is 80 Ma. The coincidence of pressure during crystallization, deduced for this granodiorite from aluminum in hornblende, with pressure deduced for peak metamorphism from mineral assemblages in pelitic rocks suggests a Mesozoic age for regional amphibolite facies dynamothermal metamorphism. The sequential development of the aluminous assemblage staurolite, kyanite, and sillimanite + muscovite appears to precede D2 during an interkinematic period. The deformation of high-grade index minerals (sillimanite, staurolite, and kyanite) and the overprinting of crenulated sillimanite by annealed or recrystallized D2 crenulated micas suggest that recrystallization accompanied or outlasted D2. D1, which developed the fabric within which D2 minerals grew, may be more than one event, including thrust stacking perhaps in the Early Cretaceous, shearing during extension or compression in the Precambrian, and mineral growth during burial by younger Precambrian and Paleozoic sediments.

INTRODUCTION

The Elk City area (Figure 1) occupies a critical position in recording central Idaho's geologic history from the Proterozoic through the Eocene. This report covers the Elk City, Black Hawk Mountain, Lick Point, Anderson Butte, and the southern parts of the Selway Falls and Stillman Point 7.5-minute quadrangles (Figure 2). This is the north-central part of the area mapped by the Idaho Geological Survey during the summer of 1989 (Lewis and others, 1990), which spans the Clearwater orogenic zone of Reid (1959). Exposed are high-grade metamorphic

[1]Idaho Geological Survey, University of Idaho, Moscow, ID 83844-3014
[2]Present address: Division of Geology and Earth Resources Division, Washington State Department of Natural Resources, 1111 Washington Street SE, Olympia, WA 98504-7007
[3]Department of Geology, Western Washington University, Bellingham, WA 98225-9080

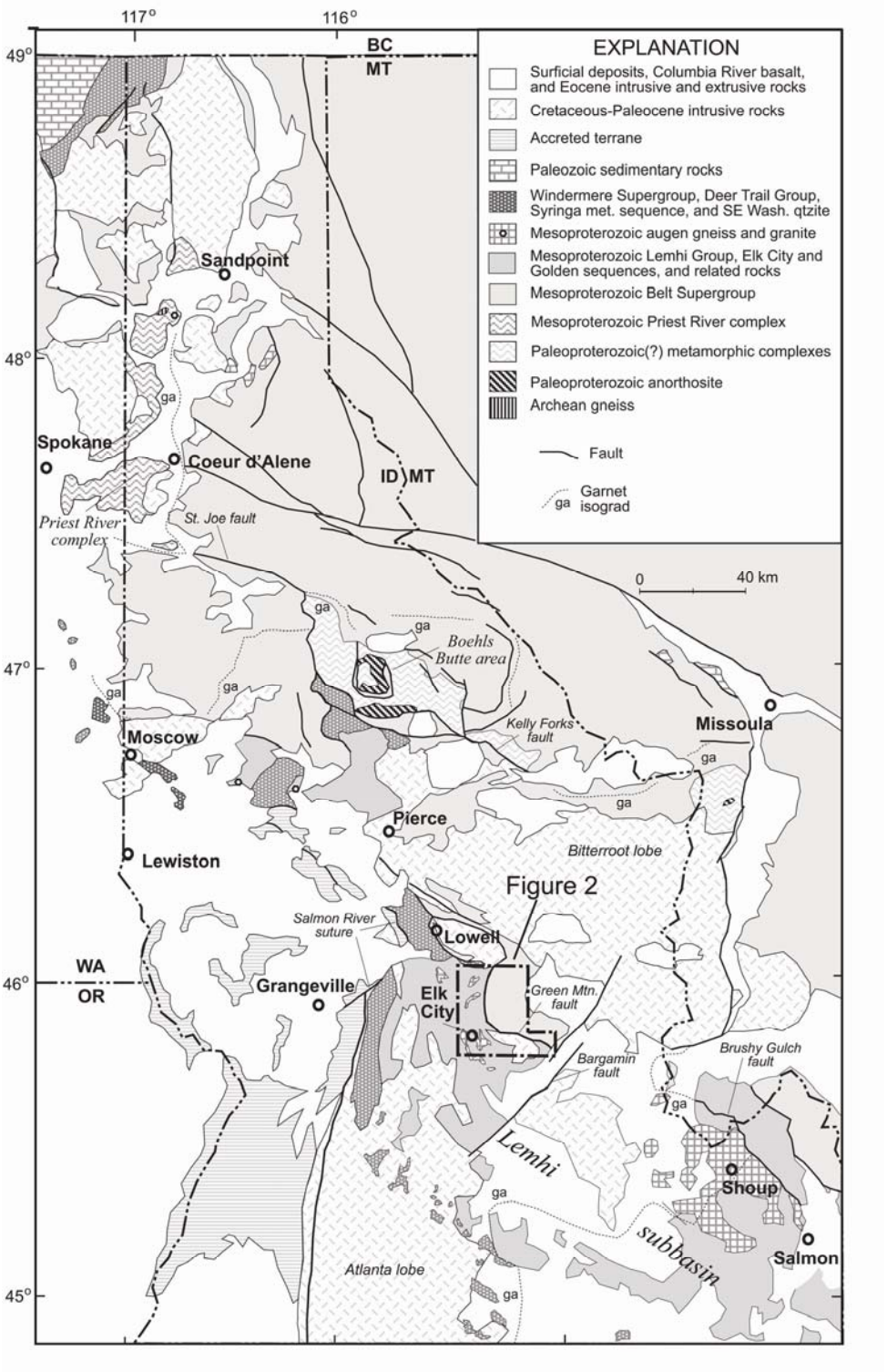

Figure 1. Generalized geologic map of northern Idaho showing area of study between the Atlanta and Bitterroot lobes of the Idaho batholith. The study area (outlined) is in the sillimanite-muscovite zone of the upper amphibolite facies. The batholith has been named the cause of this metamorphism (Hietanen, 1962; Hamilton, 1963; Onasch, 1987; Myers, 1982) partly because of the increase in metamorphic grade toward the Bitterroot lobe.

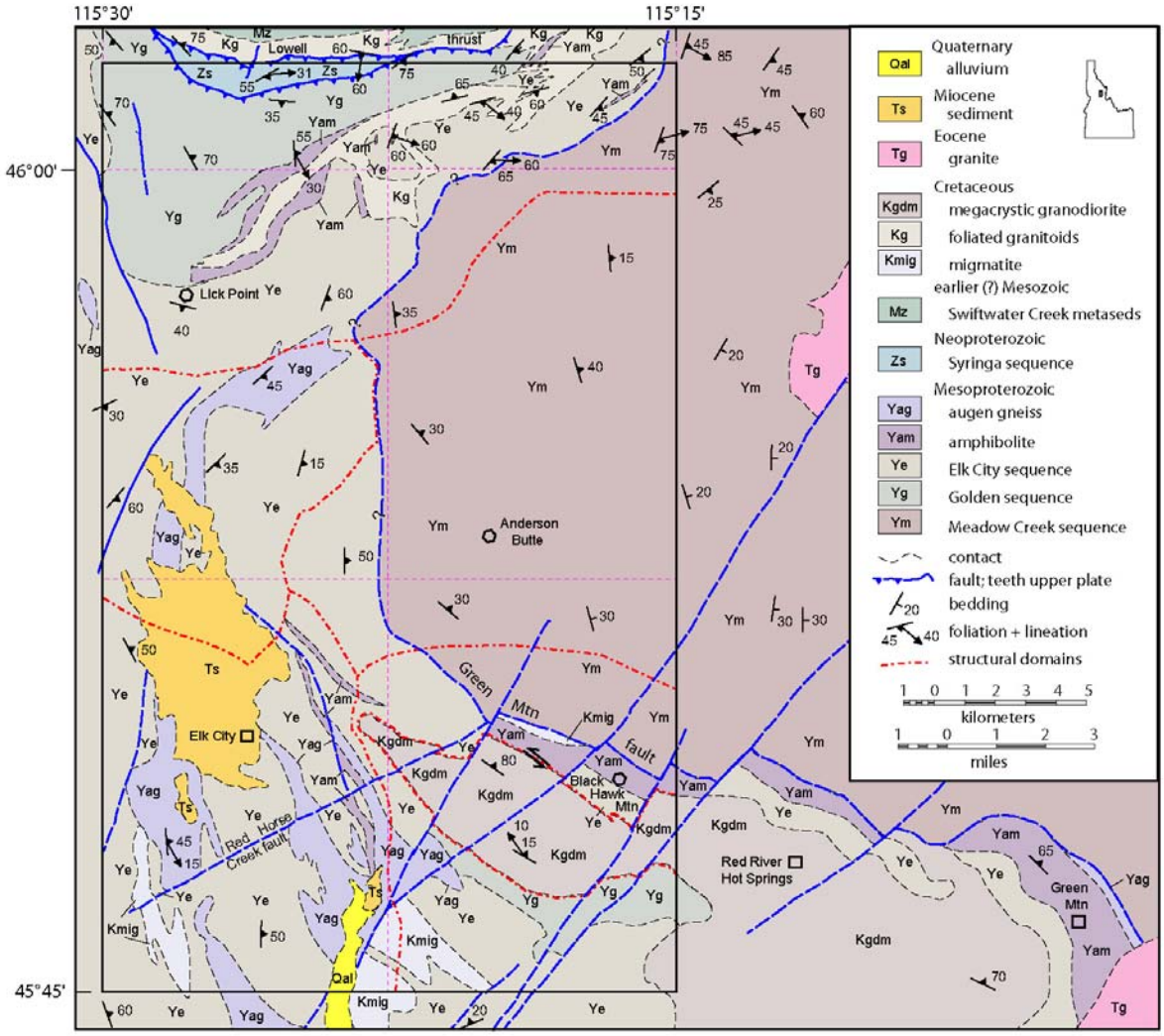

Figure 2. Simplified geologic setting of report area. Major units and symbols are in the legend. Solid rectangle is area of report; dot-dash lines are approximate boundaries of structural domains in Figures 3 and 6. Faint dashed lines outline 7.5-minute quadrangles. Based on Lewis and others (1992, 2007), Burmester and others (1992), and unpublished Idaho Geological Survey mapping.

rocks plus Cretaceous and Tertiary intrusions between the Bitterroot and Atlanta lobes of the Idaho batholith (Figures 1 and 2). Petrographic and structural analyses for this report closely followed field work. More recent geologic mapping and geochronology allow results of this structural study to be put in a useful regional perspective.

The study area includes an important but poorly understood contact or boundary. Rocks to the north and east are part of the Belt Supergroup proper, deposited 1,470-1,400 Ma (Anderson and Davis, 1995; Sears and others, 1998; Evans and others, 2000). Rocks to the southeast, south, and west (Lemhi subbasin on Figure 1) have been correlated with the Belt (such as Shenon and Reed, 1934; Reid and others, 1970; Doughty and Chamberlain, 1996; Winston and others, 1999; Tysdal, 2000). They are similar to upper Belt strata in detrital zircon minimum ages and age spectra (Lewis and others, 2007c; Link and others, 2007) and Sm-Nd analysis (Doughty and Chamberlain, 1996). The southwest rocks, however, are distinct. They host 1,380-1,370 Ma A-type granite and mafic intrusions (now mostly augen gneiss and amphibolite) and are associated with Neoproterozoic rocks correlated with the Windermere Supergroup (Lund and others, 2003). Belt Supergroup rocks have neither of these associations. This suggests that the two assemblages accumulated far enough apart or in basins subject to such different late Proterozoic tectonics that the boundary between may have accommodated large movement.

We use the term Lemhi subbasin for Lemhi Group strata near Salmon and higher grade versions near Elk City (Figure 1), modifying the terminology of O'Neill and others (2007) who referred to them as the Lemhi basin. These same rocks have been considered part of a single structural block (Hawley Creek thrust plate; Brushy Gulch-Red River thrust slab) by both Skipp (1987) and Lund and others (2004a). In the study area, we mapped the boundary as the Green Mountain fault (Figures 1 and 2). The Green Mountain fault may have a long and complex history, including left-lateral strike slip as indicated by steep mylonite fabrics with shallow stretching lineations. We interpreted earlier motion to include west vergent thrusting because higher stratigraphic level Neoproterozoic rocks are found exclusively to the west. In contrast, Lund and others (2008) called the boundary the Brushy Gulch-Red River thrust fault and favored east vergence because rocks to the west are migmatic and more deformed than rocks to the east. They also ran the north end of the fault westward south of the Lowell thrust instead of to the east.

North and northeast of the study area and north of the Bitterroot lobe, low-grade rocks of the Belt-Purcell Supergroup contain only a burial metamorphic fabric (Norwick, 1972), which increases with depth in the stratigraphic succession. In contrast, rocks in the study area are polymetamorphic and highly deformed and were intruded by Precambrian, Cretaceous, and Tertiary granitic magmas. The following seven regional events could be responsible for deformation and metamorphism in the study area:

(1) compression or extension and metamorphism during the intrusion of Proterozoic granitic and mafic magmas about 1.38 Ga;
(2) regional metamorphism and possibly deformation about 1.3-1.0 Ga;
(3) extension and possibly local intrusion during Neoproterozoic rifting;
(4) compression or transpression during the Early Cretaceous docking of outboard exotic terranes;
(5) compression during the Late Cretaceous Sevier thrusting;
(6) intrusion of the Late Cretaceous-Paleocene Idaho batholith; and
(7) extension and related magmatic activity during the Eocene.

After deposition of the Belt-Purcell Supergroup, deformation and metamorphism accompanied or preceded the intrusion of granitic magmas to the north in British Columbia (Leech, 1962; Ryan and Blenkinsop, 1971; McMechan and Price; 1982) and to the south near Salmon where they were accompanied by mafic magmas and partial melting (Evans and Zartman, 1990; Doughty and Chamberlain, 1996). Metamorphism that led to garnet growth in foliated metasediment to the northwest in the Boehls Butte area (Sha and others, 2004; Vervoort and others, 2005; Zirakparvar and others, 2006) could possibly have affected the Elk City area as well. Neoproterozoic Windermere Supergroup to the northwest in northeastern Washington (Miller, 1994) and correlative rocks south of Elk City (Lund and others, 2003) include igneous rocks and likely result from initial extensional continental breakup (Devlin and Bond, 1988). Similar age strata without an igneous component are known from west and northwest of the area of this report (Lewis and others, 2007c; Lund and others, 2008), making this Windermere-age event more widespread than previously thought. But spatial association of Neoproterozoic rocks with the Lemhi subbasin (Elk City and Golden metamorphic sequences) and not the Belt proper suggests that this event may not have affected Belt strata.

Effects from the docking of allochthonous terranes, the Sevier orogeny, and the intrusion of the Idaho batholith are not easy to separate. This period may have begun about 144 Ma at the Salmon River suture west of Elk City (Selverstone and others, 1992) with eastward propagation of magmatism and deformation through time as the orogenic wedge thickened. Near the suture southwest of the Elk City area, directional metamorphic fabric was developed and deformed in as many as four episodes; maximum metamorphic conditions are dated at 118 Ma, with possible subsequent dynamothermal events at 109 and 101 Ma, and a last at 93 Ma coincident with the intrusion of tonalite magmas (Lund and Snee, 1988). Prograde metamorphism may have later reached northwest of Elk City (90-87 Ma; Lewis and others, 2007c) and the northern margin of the Bitterroot lobe of the Idaho batholith northeast of Elk City (100-80 Ma; M1; House and others, 1997). Early tonalite and quartz diorite phases of the Idaho batholith have similar or slightly older ages (Lewis and others, 1987; and ones cited in Lewis and others, 2005; 2007b; Russell and Gabites, 2005). These are foliated parallel to fabric in the country rock, indicating that widespread penetrative strain dates from or postdates their intrusion. Regional contraction appears to have been consistently east-northeast (Bird, 1998, 2002). The characterization that the Salmon River suture formed during dextral transpression (Lund and Snee, 1988) is consistent with this.

North of the Elk City area, the suture between arc and continental crust is not as sharp as elsewhere. A Late Cretaceous metasedimentary unit with arc provenance and 78 Ma and 70 Ma metamorphic ages was intruded by an 86 Ma trondhjemite that lacks inheritance from Laurentia (Lund and others, 2008). This intrusion and a 73 Ma granodiorite with inheritance from continental and young sources are penetratively deformed and have 68-60 Ma metamorphic ages (Lund and others, 2008). Several shear zones strike west-northwest from or beyond there (Lewis and others, 2005; Lewis and others, 2007a). One of these includes a deformed 73 Ma pluton (Payne, 2004; McClelland and Oldow, 2007). This suggests that localized intense deformation postdated 73 Ma and was possibly as young as the youngest metamorphic age of 60 Ma (Lund and others, 2008). Also arrayed along and southwest of these shear zones are Neoproterozoic rocks of the Syringa metamorphic sequence (Lewis and others, 2007a; Lund and others, 2008). The easternmost Syringa and Mesozoic arc rocks and the east end of the west-northwest shear zones are just north of the Elk City area. In between that and the north end of where the Green Mountain fault zone is best defined is a complicated region of mixed metasedimentary and metaigneous rocks (paragneiss and schist and tonalitic orthogneiss). The Green Mountain fault zone and the shear zones to the northwest likely were once continuous through this region.

Southwest of Elk City, rocks now at the surface appear to have been cool and at 4-9 km depth during emplacement of main phase plutons about 74 Ma and subsequent quartz veining at 71 Ma (Lund and others, 1986). In contrast, peak metamorphism and anatectic melting northeast of the Elk City area was from 64 Ma to 56 Ma (M2; House and others, 1997), but that may have marked the end of contractional deformation and closely preceded extension (House and others, 2002). Plutonic rock with little or no fabric may date from this time and result at least in part from partial melting of the thickened orogenic wedge. The orogenic wedge's collapse during Eocene extension may be more compressed in time than its contraction, but similarly dependent on location and depth (e.g., House and others, 2002). Expected local effects, however, likely are narrow mylonite zones, perhaps within syn-extensional dikes.

LITHOLOGIC UNITS

Rocks in the Red River Hot Springs-Elk City area are described in Lewis and others (1990), Burmester and others (1990), and Lewis and others (1998) and those to the north in Lewis and others (2007a). The brief descriptions below are intended to emphasize mineral assemblages and relations critical to our interpretations. Hosted by metasedimentary rock, the igneous units of the area are the basis for understanding the timing of and conditions during their intrusion. These units are the augen gneiss of Red River, a superficially similar megacrystic granodiorite, amphibolite, and migmatite. The metasedimentary units contain different proportions of biotite gneiss, schist, quartzite, and calc-silicate. All have pelitic layers that locally contain sillimanite and rarely garnet. Only some of the units contain sillimanite and kyanite. These units span the area and provide the basis for using mineral equilibria to deduce petrogenesis.

AUGEN GNEISS OF RED RIVER

The augen gneiss of Red River (Greenwood, 1967) is exposed both north and south of Elk City (Figure 1; *Yag*, Figure 2). It contains alkali feldspar megacrysts, commonly rimmed with plagioclase, and smaller plagioclase phenocrysts in a groundmass of biotite, quartz and feld-

spar. Megacrysts range from nonstrained euhedral without strain shadows to more strained augen with asymmetric strain shadows. The least-strained samples of the augen gneiss are indistinguishable from strained samples of Proterozoic porphyritic granite south of Shoup.

The augen gneiss of Red River has been dated at 1,525 ± 82 Ma (Reid and others, 1970) and 1,370 Ma ± 100 Ma (Evans and Fischer, 1986) using U-Pb methods. Excess radiogenic lead (Reid and others, 1970; Evans and Fischer, 1986; Evans and Zartman, 1990) accounts for the large uncertainty in age (Evans and Fischer, 1986). Because it probably is genetically related to porphyritic granite and augen gneiss near Shoup, the more precise ages of 1,370 ± 10 Ma from the Salmon area (Evans and Zartman, 1990) and 1,379 ± 12 Ma from west-northwest of Pierce (Lewis and others, 2007c) appear applicable to this unit in the Elk City area. Chemical characteristics are similar to those of A-type (anorogenic) granites of similar age elsewhere in the western United States (Anderson, 1983).

AMPHIBOLITE

Amphibolite occurs in a large mass at Green Mountain, southeast of Elk City (*Yam*; Figure 2), and as many other bodies, some too small to show on Figure 2. Most amphibolite is probably cogenetic with the augen gneiss and part of the basalt-granite bimodal suite found to the south (Evans and Zartman, 1990; Doughty and Chamberlain, 1996). The amphibolite is typically associated with 20 to 60 percent strained granitic interlayers and fragments of mylonitized quartzite and augen gneiss. This association suggests tectonic mixing in the Green Mountain fault zone or its earlier incarnation. That the granitic material is unlike the augen gneiss suggests the fault and possibly some of the amphibolite are Cretaceous in age.

MEGACRYSTIC GRANODIORITE

The megacrystic granodiorite is exposed in a large pluton east of Elk City (*Kgdm*; Figure 2). The unit is hornblende- and biotite-bearing with accessory sphene, magnetite, and allanite-cored epidote. The granodiorite is typified by alkali feldspar megacrysts 2-6 cm long. Mineral alignment ranges from rare, moderately developed igneous flow foliation to strong L-S fabric defined by aligned hornblende, biotite, plagioclase, and phenocrysts of alkali feldspar. Petrographic evidence for plastic flow documents that some deformation was magmatic, but its rarity suggests most was submagmatic. Pressure calculated from the aluminum content of hornblende in two samples from the Black Hawk Mountain area averaged 8.9 ± 1 Kb (Hirt and Dragovich, 1990), which is consistent with the high pressure of soldification suggested by apparently magmatic epidote (Zen and Hammarstrom, 1984; Zen, 1985). A $^{40}Ar/^{39}Ar$ plateau age of 80.5 ± 0.3 Ma on hornblende (L.W. Snee, oral commun., 1991) for a single sample probably dates cooling below 500°C. Nevertheless, the megacrystic granodiorite in the Elk City region appears to have the same mineral and chemical composition as a porphyritic granodiorite mapped in a northwest-southeast swath across much of the Atlanta lobe; samples of that rock yielded a U-Pb zircon age of 88 ± 6 Ma and a K/Ar hornblende age of 84.7 ± 2.9 Ma (Lewis and others, 1987). It also is similar to early-phase megacrystic granitoids in the Bitterroot lobe (Hyndman, 1989; Lewis and others, 1992b), one of which has a U-Pb SHRIMP date of 94 ± 1 Ma (Lund and others, 2008). Correlation of the megacrystic granodiorite exposures near Black Hawk Mountain and Red River Hot Springs with the Precambrian augen gneiss by Greenwood (1967) and Greenwood and Morrison (1973) may have contributed to the difference between their tectonic interpretation and ours.

PROTEROZOIC METASEDIMENTARY ROCKS AND MIGMATITE

Much of the Elk City area is underlain by the amphibolite facies Elk City metamorphic sequence (*Ye*; Figure 2), a mixed unit consisting largely of quartz-rich biotite gneiss and biotite schist, along with minor amounts of calc-silicate rock and plagioclase-rich quartzite. The sequence is distinguished by abundant gneiss and cm-scale lenses of sillimanite and muscovite scattered within the schist. Detrital zircon analyses of this rock at Dutch Oven Creek 9 km west of Elk City indicate a Mesoproterozoic (upper Belt Supergroup equivalent) age (Lund and others, 2008). The Golden metamorphic sequence (*Yg*; Figure 2) of feldspathic quartzite gneiss and schist is interpreted to underlie the Elk City rocks. Northeast of the Elk City sequence is the Meadow Creek metamorphic sequence (*Ym*; Figure 2), which consists of quartzite, muscovitic quartzite, muscovitic schist, and minor calc-silicate rocks. The sequence is distinguished by abundant quartzite and muscovite, preserved sedimentary structures in some of the quartzite and calc-silicate, and no augen gneiss or amphibolite. The unit is possibly equivalent to the Missoula Group of the Belt Supergroup.

Migmatite (*Kmig*, Figure 2) is present locally. The magmatic material is generally nondeformed leucocratic granodiorite and likely Late Cretaceous or Paleocene in age, because it resembles the biotite granodiorite of the

Idaho batholith. Melanosomes constitute 30 to 60 percent of the rock. Their distribution, with abundant biotite gneiss, less common schist and augen gneiss, and rare calc-silicates, parallels abundances of mapped lithologies. The foliation and folds in most melanosomes have attitudes similar to regional trends, which is consistent with the passive emplacement of the granitic material after ductile deformation and metamorphism had ceased. But in other occurrences, especially near the megacrystic granodiorite, the foliation and lineation of the granitic material, and the biotite selvages around melanosomes indicate partial melting or assimilation during deformation.

The Syringa metamorphic sequence (*Zs*; Figure 2) of coarse, feldspar-poor quartzite, schist, and calc-silicate rocks is barely in the report area, but its presence, and that of arc-affinity sedimentary rocks to the north (*Mz*; Figure 2), document the juxtaposition of young rocks against the Proterozoic sequences along the Lowell thrust (Lund and others, 2008) and related faults.

STRUCTURAL FEATURES

Four deformations have been recognized in the Elk City and surrounding region from the orientations of folds and foliations and the intensity of their development (Reid, 1959; Greenwood, 1967; Morrison, 1968; Reid and others, 1973; Clark, 1973; Wiswall, 1979; Reid, 1987; Wiswall and Hyndman; 1987; Bittner, 1987). There is general agreement on the style of D4, but D1, D2 and D3 structures vary in development and orientation through the region. We agree that the region's history can be described by these four major deformational events, although we question some of the previous interpretations about the absolute timing of the first and second deformations. For completeness, we add a faulting event between D2 and D3, and a fifth event of Miocene faulting.

Our analysis is based on field measurements and oriented samples collected in 1989 and data from Reid (1959). Assigning fabrics to the early deformations is based on field observations of cross-cutting relations, measurements of orientations of foliation, lineation and fold axes, and petrographic analysis of 120 thin sections cut parallel to the XY, YZ and XZ planes of the commonly well-lineated tectonite fabrics. The XY plane was taken as the regional foliation (S1) with X defined as the L2 direction. Local similarities in structural styles and attitudes of S1 foliations and L2 lineations were used to divide the area into seven structural domains (Figure 3). A brief comparison of our observations with those of previous workers, along with a description of each of the deformational stages, is presented below.

FIRST DEFORMATION (D1)

The S1 foliation, defined by micas, is parallel or subparallel to compositional layering (S0) except in the hinges of rare F1 folds where the S1 foliation is axial planar to folded bedding in metasedimentary rock units (Reid, 1959). F1 folds are recumbent and isoclinal and have sharp hinges, high amplitude to wavelength ratios, and similar style (Reid, 1959; Greenwood, 1967). Most are small (<5m), but a few are reported to be large (Greenwood and Morrison, 1973). A similar deformation style has been reported elsewhere in the high-grade schists and gneisses of central Idaho (Morrison, 1968; Reid and others, 1973; Standish, 1973; Chase, 1973; Wiswall, 1979; Bittner, 1987; Hyndman and others, 1988) and appears to be regional in extent. A common theme related to D1 kinematics is that F1 folds appear to be rare in the region (Morrison, 1968; Hyndman, 1989).

The orientation of the rare F1 folds remains poorly determined. The available observations suggest F1 folds trend northwest-southeast and verge to the southwest (Reid, 1959; Greenwood, 1967). The S1 foliation, although steepened in dip by later deformations, appears to have been initially flat lying or recumbent (Reid, 1959).

S1 Foliation and F1 Folds

The dominant fabric attributable to the first deformation is the pervasive S1 foliation, which generally strikes northwest and dips moderately to gently northeast (Figure 3). The subparallel nature of the S1 foliation and compositional layering observed at the outcrop also is evident in parallelism of the rock unit contacts and foliation patterns (Figure 2). S1 is indistinct or absent in calc-silicate and quartzite of the Meadow Creek unit, and F1 is unknown from that entire unit.

We defined F1 folds as those having S1 axial planar to folded bedding. The few we observed were isoclinal and sharp-hinged. The paucity of F1 folds, the general inability to observe these folds in three dimensions, and the imprecision in correcting their attitudes for reorientation during later deformations make it impossible to include their orientations in a structural story. The repetition of metasedimentary rock units in a manner that can be attributed to large F1 folds also was not observed, indicat-

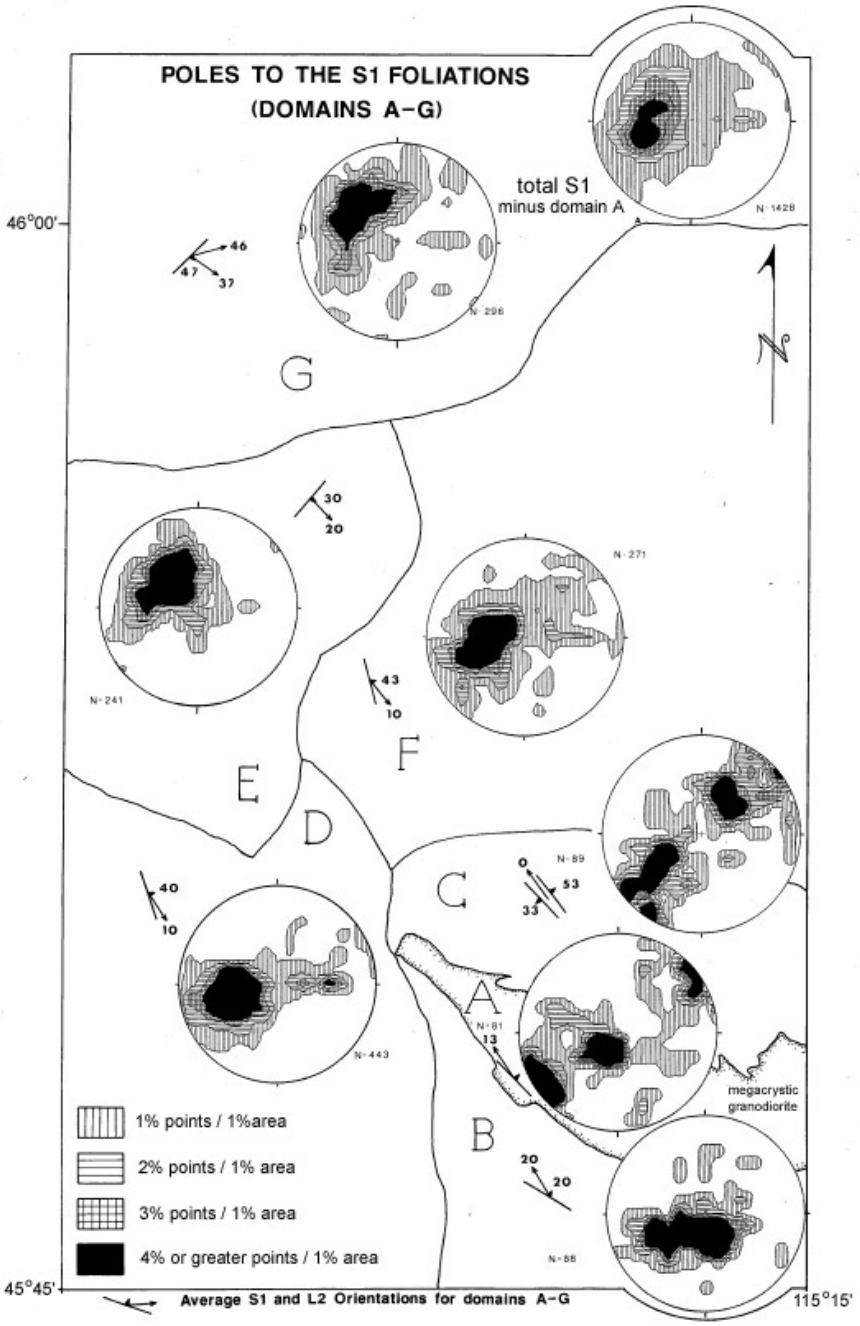

Figure 3. Lower hemisphere equal-area projections of poles to S1 foliations for domains A-G. The analysis covers only the western part of Figure 2. The average orientation for S1 in each domain is shown by the strike and dip symbols; the average trend and plunge for L2 lineations (Figure 6) are shown by the accompanying arrow. Domain A is the megacrystic granodiorite, which is excluded from the plot of all attitudes (Total S1). However, the overall average north-striking and moderately east-dipping attitude obscures the nearly continuous change in strike of foliations from northwest in southern domains B and C to northeast in northern domains E and G. This systematic change likely results from F3 or F4 warping. The greatest departure from a homoclinal east dip is in domain C, where a girdle distribution with a northwest-trending beta axis parallel to the subhorizontal L2 lineation indicates large-scale F2 folding around the beta axis. Domain C contains a well-defined antiform that may be parasitic to a larger F2 fold. The apparent girdle distribution of the foliations in domain A likely results from the inclusion of a later vertical cleavage in the granite along with a more horizontal fabric developed parallel to S1. The low-dip fabric is interpreted to be tectonic and a result of deformation during intrusion.

ing that F1 folds are probably intraformational. The lack of evidence for large F1 folds makes it likely that D1 was dominated by shearing that placed bedding subparallel to S1, as was suggested for the St. Joe area to the north (Reid and others, 1981), and did not involve the formation of nappes.

D1 Microstructures and Porphyroblasts

The S1 alignment of biotite and muscovite suggests a minimum of greenschist facies metamorphism during D1. Sillimanite and kyanite also are commonly aligned in the S1 foliation (Figure 4), which suggests synkinematic D1 crystallization (Reid, 1959; Greenwood, 1967; Reid and others, 1973). Porphyroblasts inclined to the S1 foliation at various angles, although less common, suggest other interpretations are possible. These are presented below.

SECOND DEFORMATION (D2)

There is some disparity in descriptions of F2 folds by previous workers. According to Reid (1959), S1 foliation was deformed during D2 into open, isoclinal F2 folds that are upright or overturned to the west-southwest. Other workers described them as recumbent (Greenwood, 1967), upright and isoclinal (Morrison, 1968), and tight, similar and parallel shear folds (Wiswall and Hyndman, 1987). F2 fold hinges commonly contain a poorly to moderately developed axial planar foliation (S2) defined by muscovite and biotite (Reid, 1959; Greenwood, 1967; Reid, and others, 1973). Outside of the F2 hinge zones, D2 deformation appears to have utilized the anisotropy created by the S1 foliation (Reid, 1959).

We defined F2 folds as tight folds of S1 that have little or no axial planar S2 foliation. They are developed throughout the study area, particularly in the metasedimentary and augen gneiss rock units (Figure 3). They are generally inclined or overturned to the west-southwest. The attitude of their limbs is that of the S1 foliation. The average attitude of S1 (Figure 3, total S1) is similar to Reid's (1959) total S1. This average attitude and partial girdle are consistent with folding of S1 about the average F2 fold axis (Figure 5). But subdividing the study area into smaller units shows that individual, relatively homogeneous structural domains have distinct S1 foliation attitudes (Figure 3). This interdomain variation is ascribed below to later deformation.

F2 fold axes are paralleled by L2 crenulation, mineral, and stretching lineations, which also vary in attitude from domain to domain (Figure 6). A crenulated S1 foliation is generally conspicuous in the field, although coarse recrystallization of the micas obscures it in thin sections (Figures 7, 8,and 9). L2 mineral and stretching lineations are defined by (1) the alignment of hornblende prisms in the amphibolites (Figure 10b); (2) the asymmetric strain shadows behind aligned feldspar augen in the augen gneiss of Red River and aligned potassium feldspar megacrysts, which commonly contain asymmetric strain shadows, in the megacrystic granodiorite (Figure 11); and (3) the preferred orientation of micas (Figure 12) and sillimanite, and rarely of kyanite (Figure 13) in metasedimentary rocks.

Observations that (1) the crenulations parallel the F2 fold axes (compare Figures 4 and 5) and (2) the structural element being crenulated is the S1 foliation indicate that crenulations are D2. In this interpretation, we differ with Reid (1959) who suggested that the F2 fold axes bear differently than the crenulation lineations, which he stated parallel the F1 folds.

The existence of large F2 folds is suggested by the interpretation that small F2 folds as S, M and Z folds are parasitic to larger ones. Only one, however, is documented by repetition of rock units. The S1 foliations in Domain C (Figure 3), north of the megacrystic granodiorite, show an anomalous northeast-southwest girdle distribution with a shallow, northwest-trending beta axis. This beta axis parallels the L2 lineations (Figure 6; Domain C) and the small F2 folds (Figure 5). This suggests that the beta axis is the fold axis of a large, upright F2 antiform. This large fold, which is generally defined by northeasterly dips on the northeast and southwesterly dips on the southwest, may be parasitic to the large fold defined by the repetition of the schist and quartzite unit and the amphibolite unit. The megacrystic granodiorite appears to core this fold and may be responsible for its anomalous upright geometry. Alternatively, the folding in Domain C may merely reflect high strain near the post D2 fault (see below).

Relation of the Megacrystic Granodiorite to D2

The megacrystic granodiorite contains a moderately to well-developed L-S fabric. The lineation in this granitic body is defined by aligned potassium feldspar megacrysts, hornblende, and biotite. The structural domains that border the megacrystic granite (Domains B and C) contain L2 lineations and S1 foliations that parallel the lineations and foliations in the megacrystic granodiorite (Figures 3 and 6). The following relations suggest that the megacrystic granodiorite is syntectonic with respect to D2:

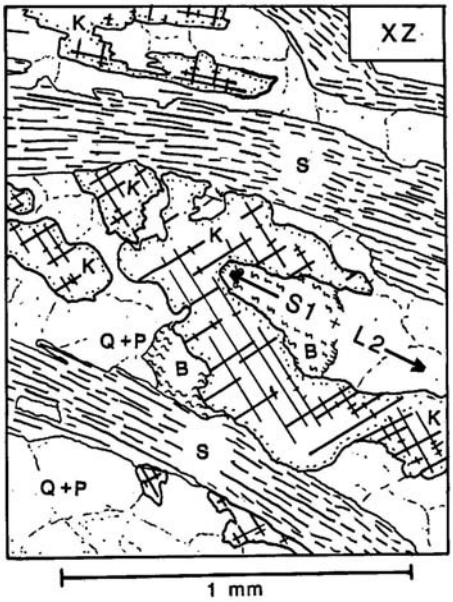

Figure 4. Sketch of biotite gneiss thin section with sillimanite (S) coexisting with kyanite (K) within S1. This, taken alone, suggests crystallization during D1. The lack of definitive overprinting relationships in this and other samples suggests that kyanite and sillimanite were stable during crystallization and formed under conditions near their reaction boundary. The quartz and plagioclase matrix (Q + P) has nonsutured and polygonal, low-strain geometry suggestive of a low-strain environment or recrystallization.

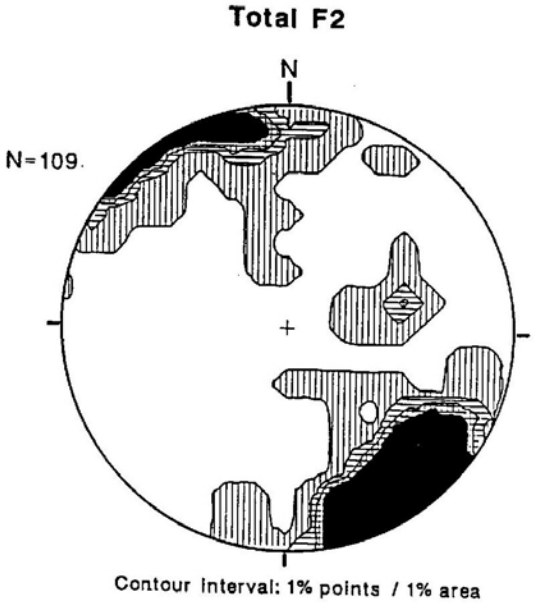

Figure 5. Lower hemisphere equal-area projection of mesoscopic F2 fold axes from all domains shows a distinct, subhorizontal, northwest-southeast orientation. The F2 fold axes parallel the L2 lineations (Figure 6). Variation in attitudes probably is due to later deformation.

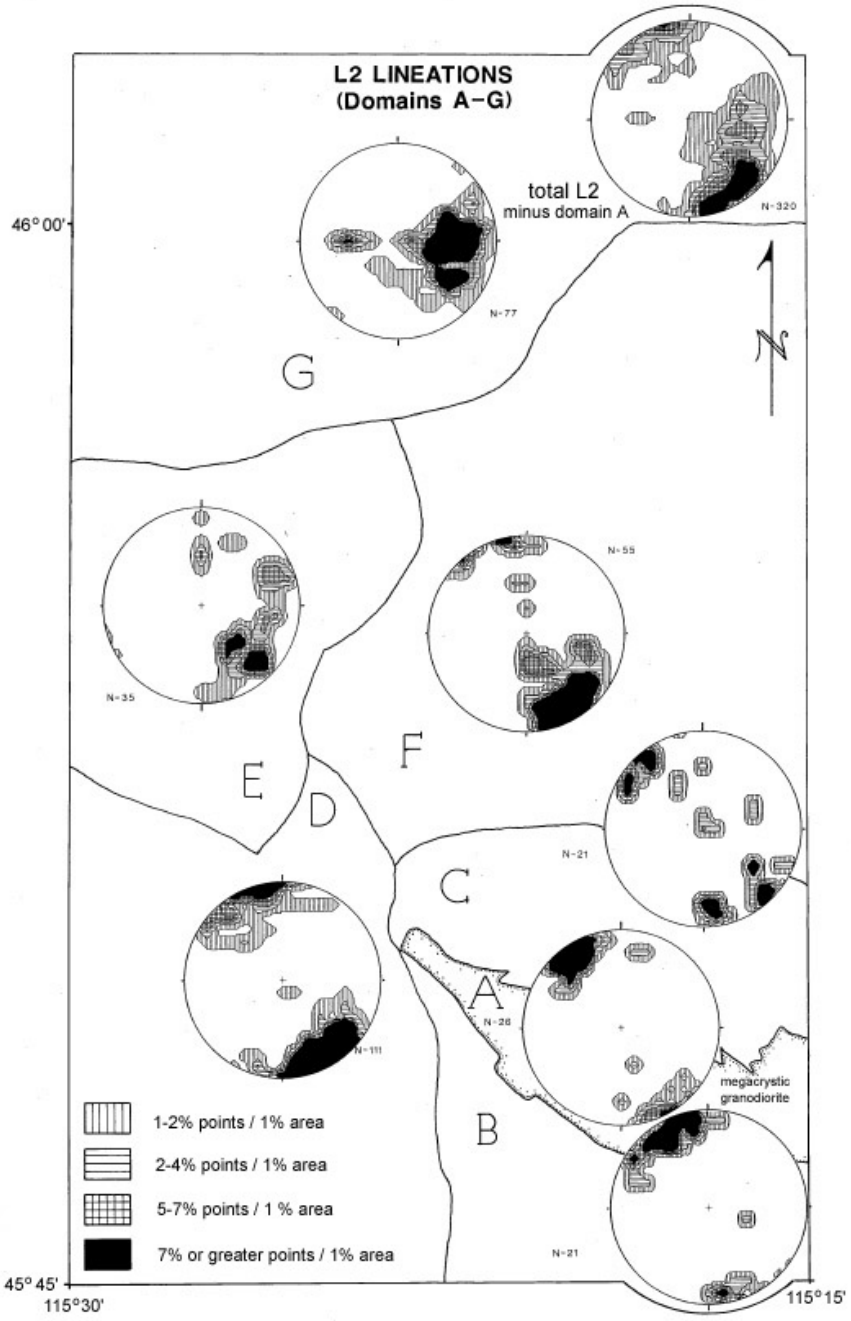

Figure 6. Lower hemisphere equal-area projections of the L2 lineations from individual domains A-G and all domains (Total L2) excluding domain A, the megacrystic granodiorite. Area covered is the same as in Figure 3. L2 mineral lineations in the metasediments are defined by micas and sillimanite and in the amphibolites by hornblende. L2 mineral lineations in the megacrystic granodiorite are defined by hornblende and biotite and by strain shadows behind plagioclase and potassium feldspar megacrysts. Northwest-southeast subhorizontal L2 lineations in domains B to F parallel the lineation in domain A. This parallelism and the lack of subsolidus recrystallization in the megacrystic granodiorite suggest that the formation of L2 overlapped the intrusion of the megacrystic granodiorite. The anomalously steep, easterly plunging lineation in domain G, the partial girdle in domain E, and the multiple modes in domain C probably reflect later folding, but may be due in part to the inclusion of more than one age of lineation.

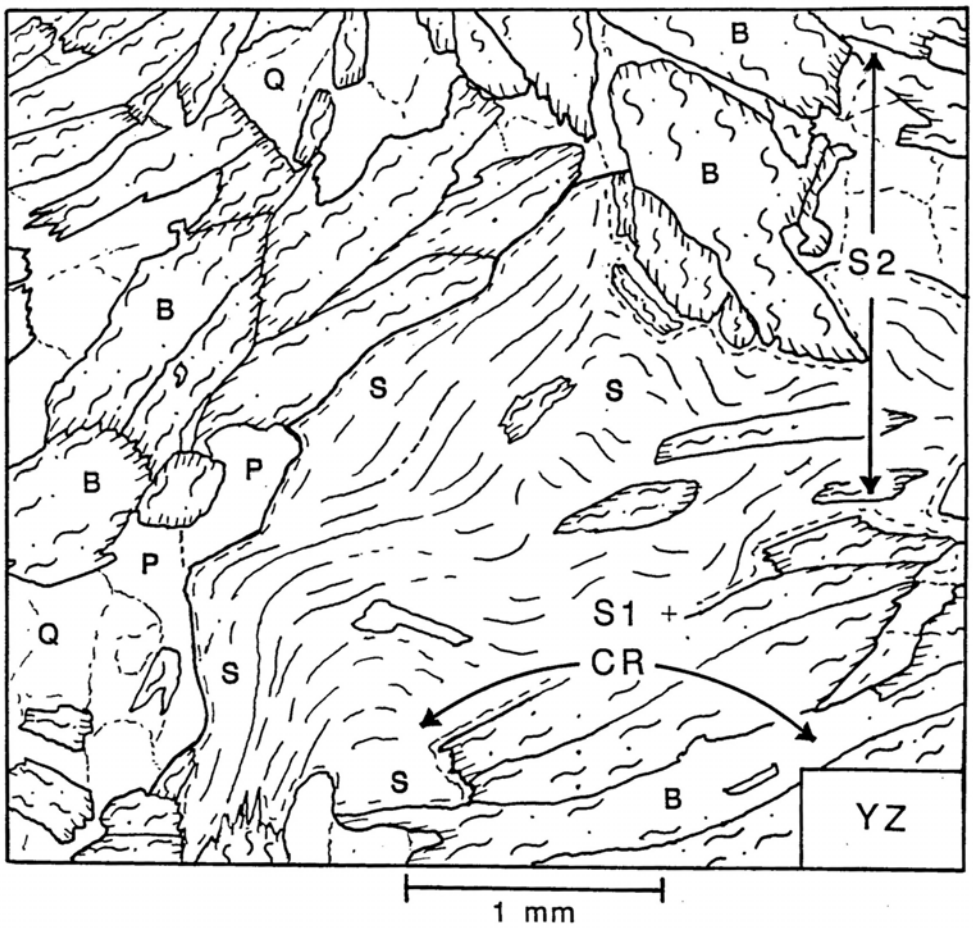

Figure 7. Sketch of sillimanite-biotite schist thin section cut perpendicular to the L2 lineation (X). The L2 crenulation is defined macroscopically by biotite and sillimanite. Local inclination of biotite (B) with straight extinction to the S1 foliation indicates crenulated biotite was coarsely recrystallized. Crenulated (CR) sillimanite (S) shows sweeping extinction, suggesting that sillimanite growth predates D2 and that it was not recrystallized during the second deformation.

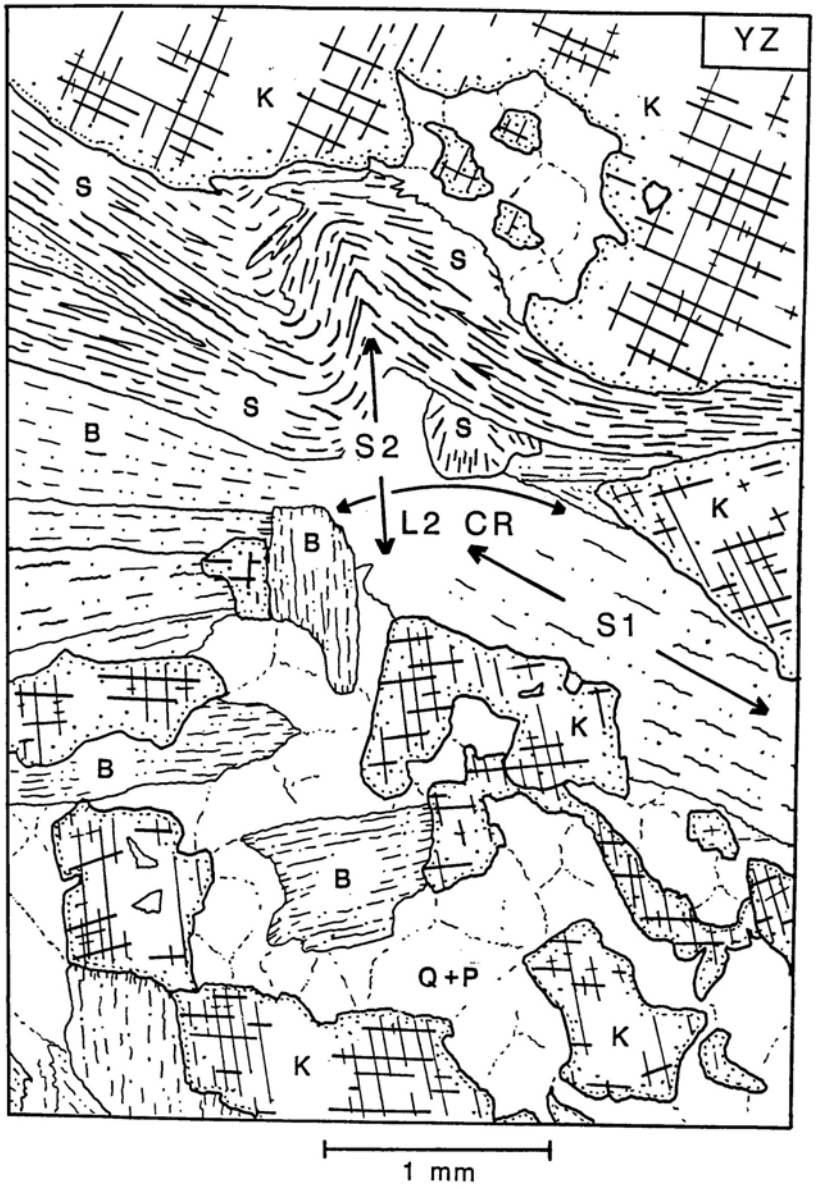

Figure 8. Sketch of kyanite-bearing quartzo-feldspathic schist thin section cut perpendicular to the S1 foliation and L2 lineation. Biotite (B) and crenulated (CR) sillimanite with sweeping extinction (S) define the S1 foliation in most places, but some biotite appears to define S2 axial planar to the crenulation. Crenulation of sillimanite indicates that sillimanite-grade metamorphism preceded the second deformation. Adjacent kyanite (K) and sillimanite appear to be in equilibrium.

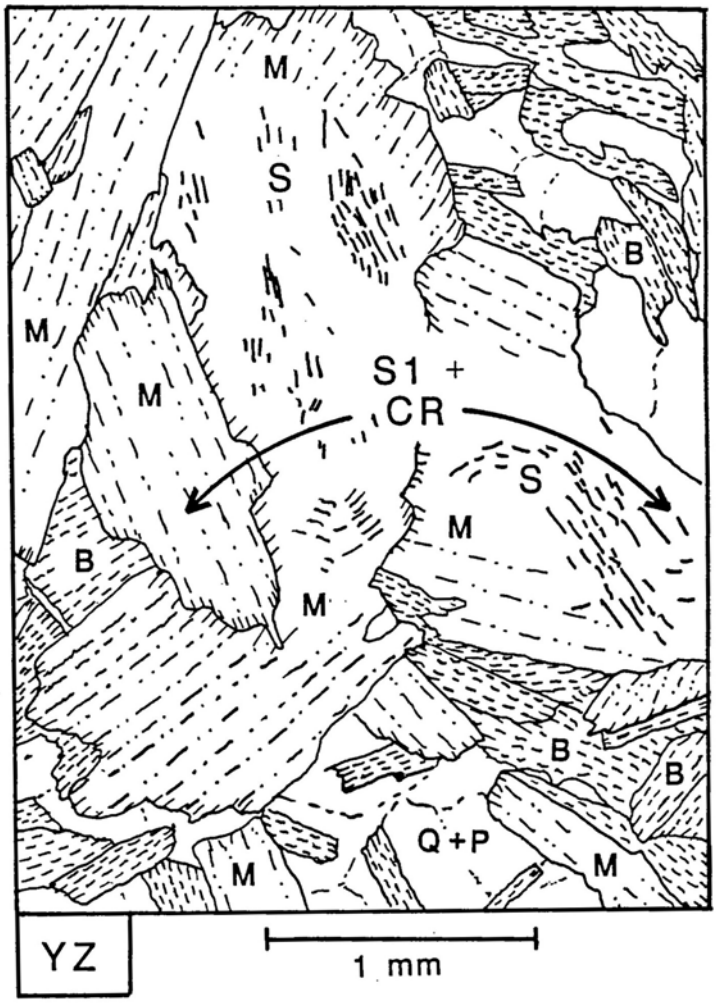

Figure 9. Sketch of sillimanite-biotite-muscovite schist thin section cut perpendicular to the S1 foliation and L2 crenulation lineation. Both muscovite (M) and biotite (B) have a macroscopic crenulation although individual grains lack sweeping extinction, indicating they have been recrystallized. The curvature of sillimanite needles (S) within the muscovite, interpreted to date from crenulation, indicates that the recrystallization of micas during D2 occurred below sillimanite grade.

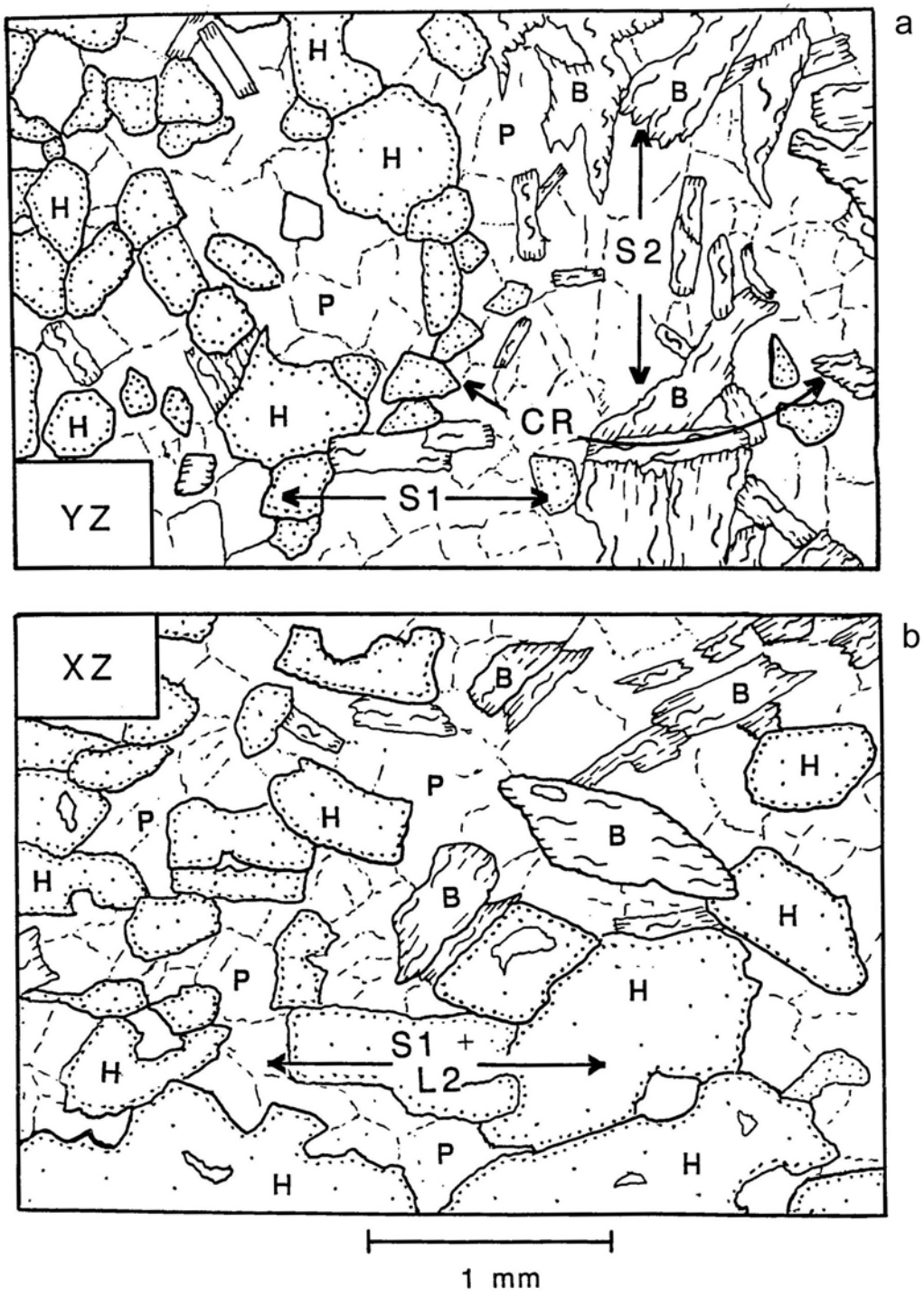

Figure 10. Sketch of amphibolite thin section cut perpendicular to the foliation and both perpendicular (a; YZ) and parallel (b; XZ) to the L2 lineation. In 10a, hornblende end-sections (H) and crenulated and recrystallized biotite (B) define the foliation, which indicates that the L2 mineral lineation observed in amphibolites is parallel to the crenulation lineation defined by folded biotite. In 10b, hornblende prisms lie along the foliation. The nonsutured plagioclase (P; oligoclase) groundmass in both thin sections shows little attenuation. The weak alignment of the hornblende prisms, as well as the lack of boudinage, suggests that the amount of shear deformation accompanying recrystallization was low.

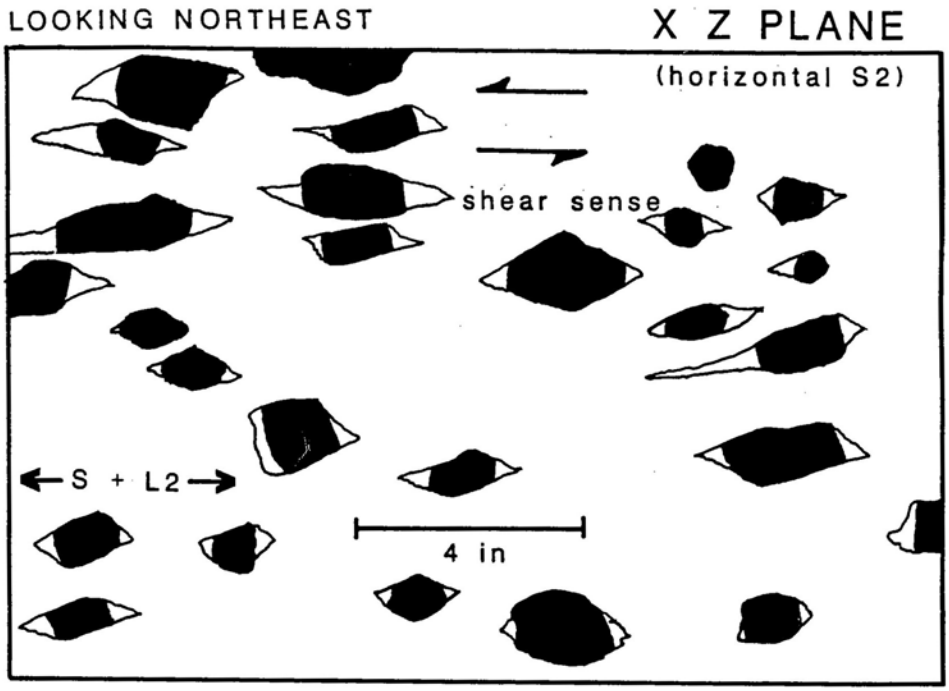

Figure 11. Sketch of megacrystic granodiorite outcrop showing asymmetry of megacryst tails that, if observed widely enough, could be used to indicate regional sense of motion.

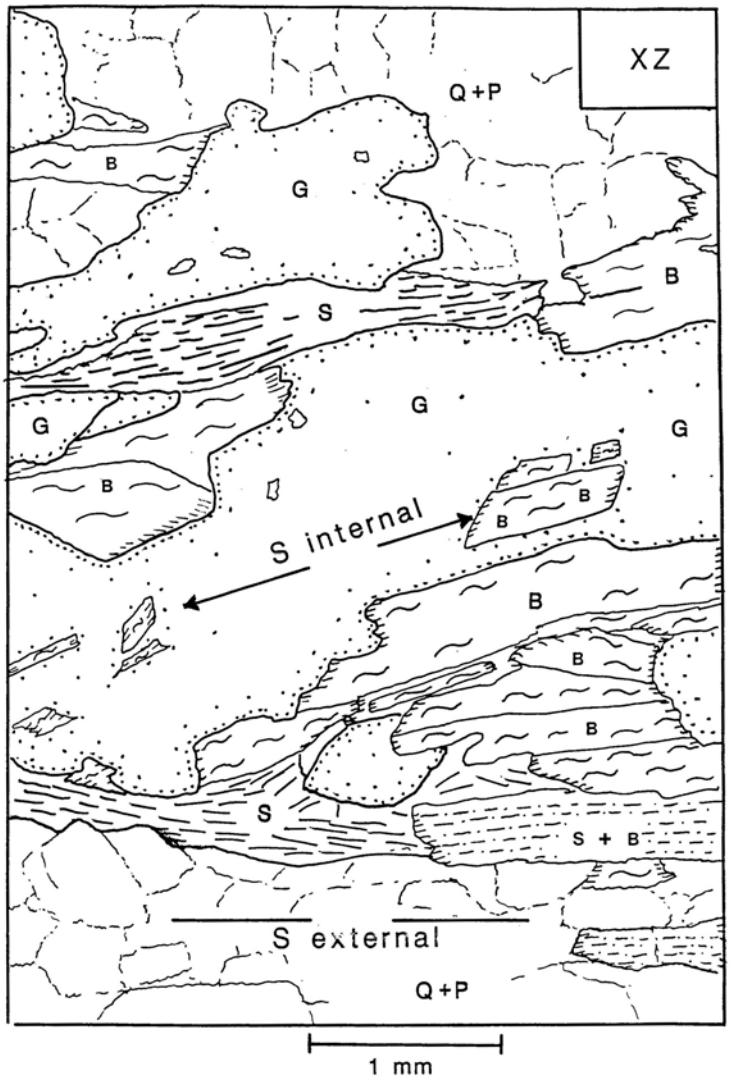

Figure 12. Sketch of garnetiferous mica schist thin section cut parallel to the L2 lineation and perpendicular to the S1 foliation. Aligned biotite (B) in garnet (G) defines an internal foliation (S internal) that is subparallel to the external foliation (S external) defined by biotite, sillimanite (S), and interleaved biotite and sillimanite (S + B). This relation indicates that garnet grew during or after formation of S1 foliation. The quartzo-feldspathic matrix (Q + P) contains stable triple junctions and does not appear strongly ellipsoidal or rodded, suggesting a low-strain environment or recrystallization.

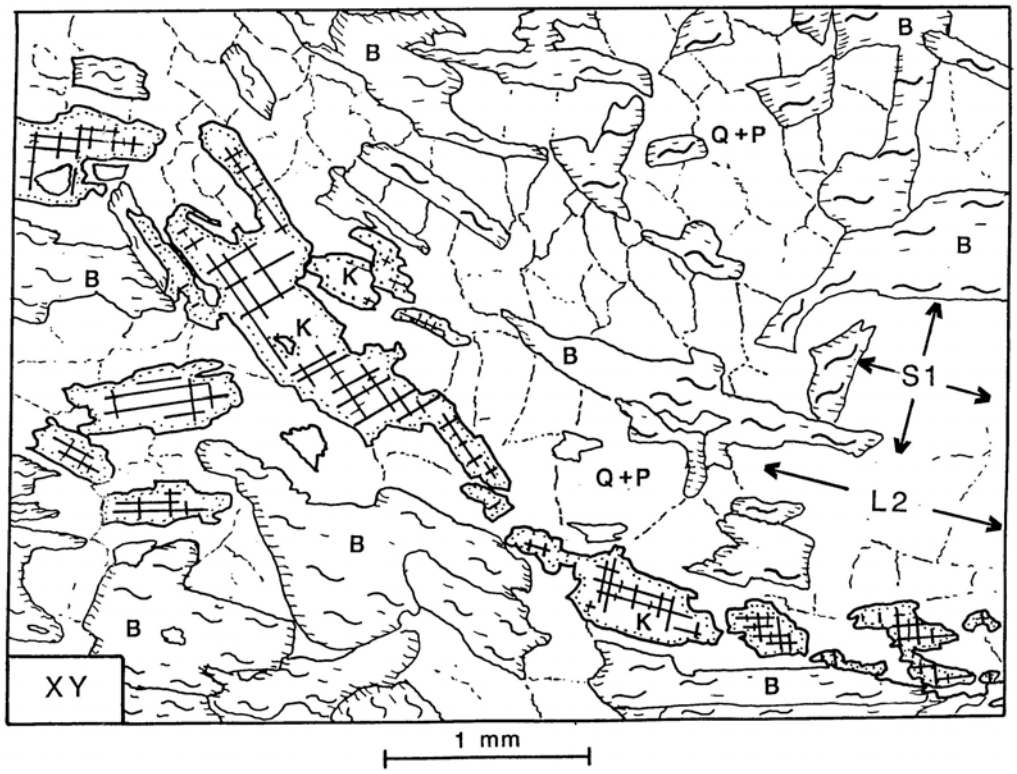

Figure 13. Sketch of thin section showing kyanite aligned with L2 in S1 foliation plane of biotite gneiss. Orientation of kyanite is attributed to D2 deformation of preexisting porphyroblasts.

(1) Both the primary igneous minerals that define the fabric and interstitial minerals show little evidence of plastic deformation. This implies that enough melt was present during deformation for crystals to rotate without significant interference from neighboring minerals (Vernon and others, 1983). This criterion is strongest where the oriented mineral is euhedral K-feldspar or plagioclase (Paterson and others, 1989). Both plagioclase and K-feldspar megacrysts are aligned parallel to the L2 lineations present in the country rocks.

(2) Quartz-filled strain shadows behind broken or boudinaged plagioclase and K-feldspar megacrysts in some samples indicate tectonic alignment of these crystals. The common orientation of megacrysts with and without asymmetric quartz-filled pressure shadows suggests that strain continued as submagmatic flow (Paterson and others, 1989) when (or where) there was less than the amount of melt necessary for magmatic flow.

(3) Foliated migmatites are spatially associated with the megacrystic granodiorite. These rocks contain felsic granitic stringers with a crystalloblastic fabric that parallels the S1 foliations (Reid, 1959) and L2 lineations in the country rocks. Reid (1959) also reported that S2 foliated and L2 lineated granitic stringers are coincident with axial planes of F2 folds. This relationship suggests that migmatization was synchronous with the development of the F2 folds, which supports the contention that magmatism was synchronous with D2 deformation.

The correlation of L2 crenulations with F2 folds and the parallelism of these elements with lineation in the megacrystic granodiorite suggest the age of D2 is Late Cretaceous, but probably no younger than the 80 Ma hornblende cooling age of the granodiorite (L.W. Snee oral, commun., 1991).

D2 Microstructures

The second deformation apparently occurred after an interkinematic period of peak metamorphism. This interpretation is supported by (1) the lack of syntectonic porphyroblast-matrix relations (e.g., snowball garnets), (2) the localized alignment of sillimanite and kyanite parallel to L2 (Figures 4 and 13), (3) the microfolding of sillimanite and fibrolite (Figures 7, 8, and 9), and (4) the apparent absence of high-grade minerals recrystallized parallel to the S2 foliation. Reid (1959) reported S2-aligned fibrolite in the study area, but we interpret fibrolite that is subparallel to the S2 foliation to be crenulation limbs because grains with anomalous extinction can be traced around hinges.

The varied recrystallization that accompanied the formation of the D2 fabric suggests deformation during the waning stages of lower amphibolite facies metamorphism. Some biotite, muscovite, hornblende, and plagioclase (oligoclase) were recrystallized during D2. Biotite and muscovite parallel S2 axial planes in some F2 hinges (Figure 8), and muscovite overprints F2 microfolded sillimanite (Figure 9). Hornblende in amphibolite also appears to have been recrystallized during this event. Hornblende prisms lack any evidence for mechanical alignment during D2 shear and appear to be recrystallized weakly parallel to L2 (Figure 10). In contrast, poikiloblastic garnets sectioned parallel to L2 and perpendicular to S1 commonly show a planar internal biotite foliation that is subparallel to S1 (Figure 12). This suggests that garnet grew after foliation formation (D1), probably during the interkinematic phase. But a thin section cut perpendicular to the L2 crenulation lineation in one sample shows garnet rims overprinting apparent crenulations, suggesting that some garnet grew during or after D2.

Bulk Strain and D2 Kinematics

The second deformation (D2) produced bulk shortening, with a component of extension parallel to the F2 fold axes and lineation. Shortening is suggested by tight F2 fold and crenulation development. Evidence for extension is found in the parallel L2 mineral lineations. The possibility of rotational strain is suggested by asymmetrical augen locally in the augen gneiss of Red River and asymmetric strain shadows in the megacrystic granodiorite (Figure 11). A thorough examination of the sense of asymmetry across the area and especially in the megacrystic granodiorite should indicate if there is a regional sense of shear (e.g., Simpson and Schmid, 1983).

D2 was inhomogeneous in intensity of development as suggested by (1) the variation of F2 fold interlimb angles from nearly isoclinal to rarely open, (2) the varied development of axial planar S2 foliation, and (3) the common preservation of radiating kyanite and sillimanite grains in regions of lower D2 strain. Shear zones in the augen gneiss of Red River and megacrystic granodiorite bodies range in width from one to several hundreds of feet.

Despite their inhomogeneous development, the dominant D2 linear structural elements, including lineations and fold axes, have a consistent attitude with shallow plunge to the north-northwest or south-southeast (Figure 6). The colinearity of these structural elements suggests cogenesis under a single transpressional regime with east-northeast to west-southwest compression and subhorizontal north-northwest to south-southeast extension.

Post D2 Fault

The Green Mountain fault is named after Green Mountain, east-southeast of Elk City (Figure 2). It separates rocks of the Elk City metamorphic sequence, augen gneiss, and amphibolite from the Meadow Creek metamorphic sequence. Although it is shown as a single line, the part from east of Elk City toward Green Mountain is a 1-km-wide swath of mixed amphibolite, foliated granitic material, and mylonitized remnants of augen gneiss and quartzite. Deformation generally increases into this zone, which includes mylonite, some with clear horizontal stretching lineations and sinistral slip kinematics. Slickensides with slickenlines on polished surfaces and rusty, highly fractured quartzite near the Meadow Creek unit attest to movement at shallower levels. We consider this to be a major fault because it separates so cleanly the Meadow Creek sequence from the rest of the rock units. It may have started as a thrust fault, but we have been unable to find evidence for that.

A simple interpretation is that this fault truncates the northeast limb of the F2 antiform cored by the megacrystic granodiorite, cutting out the Elk City biotite gneiss and schist units. A dip-slip component could have brought the Meadow Creek metamorphic sequence up on the east side. This motion could also explain the presence of coarser quartzite along the fault if the quartzite is from the Golden metamorphic sequence stratigraphically below the Elk City sequence. The spatial association of the fault with the F2 fold and D2-tectonized granitic material are consistent with reverse fault movement and east-northeast to west-southwest shortening during D2. The oblique orientation of the west-northwest trend of part of the Green Mountain fault relative to this shortening direction could have driven sinistral slip as well. But the presence of mylonitic and brittle fabrics along the fault, inconsistent with ductility demonstrated by other D2 fabrics, indicates that at least the latest motion occurred after the main ductile phase of D2.

An opposite sense of shear (dextral) was derived from Greenwood and Reid's (1969) study that overlapped the southeast corner of our area. There, flexural sigmoidal folds near this fault that postdate D2 could have formed coincident with faulting. Variations of schistosity define a fold axis plunging 45° N. 10° E. These authors interpreted their results as being consistent with a right-lateral shear couple. Dextral strike slip would accommodate shortening across the complex zone to the north, although the cause of the drastic change in stress field required is unknown. Their interpretation of the timing of this deformation, however, would have to be changed because some of what they mapped as Proterozoic augen gneiss is the Cretaceous megacrystic unit, and the intrusion that truncates the structures on the southeast is Tertiary and not Cretaceous. Truncation of the fault by the Tertiary pluton also eliminates the possibility that the fault is an Eocene detachment.

THIRD DEFORMATION (D3)

Deformation postdating D2 is shown by the partial girdle distribution of the L2 and F2 axes around a moderately plunging west-southwest-trending axis (Figures 5 and 6) and the varied attitudes of F2 axial planes (Reid, 1959). Regionally, F3 folds have been characterized as gentle and open with various attitudes including steep plunge to the southwest (Reid, 1959), isoclinal and northeast trending (Greenwood, 1967), relatively open with no axial plane schistosity (Reid and others, 1973), concentric (Reid, 1987; Hyndman and others, 1988), and evolving from similar to concentric drag folds (Wiswall and Hyndman, 1987).

F3 Folds

Mesoscopic F3 folds with wavelengths of 1-3 feet were observed to fold the L2 lineations. Most F3 folds plunge gently to moderately either northeast or southwest (Figure 14). Larger F3 folds may be responsible for much of the variation of S1, L2, and F2 attitudes across the area (Figures 3 and 6). One approach to evaluate this is to unfold the S1, F2, and L2 structural elements about an average F3 fold axis to common attitudes. Such manipulation to restore L2 and F2 to horizontal makes them nearly parallel in all domains. S1 strikes also become parallel, but S1 dips are bimodal. This bimodality of foliation dips probably reflects F2 limb attitudes. Thus, F3 appears to account for most of the variation of S1 strikes and F2 and L2 attitudes across the area. The greatest plunges of L2 and F2 axes are found toward the north. This suggests that F3 may have been in response to uplift of the arc-affinity rocks under the Lowell thrust southeast of Lowell (Figures 1 and 2) north of the map area.

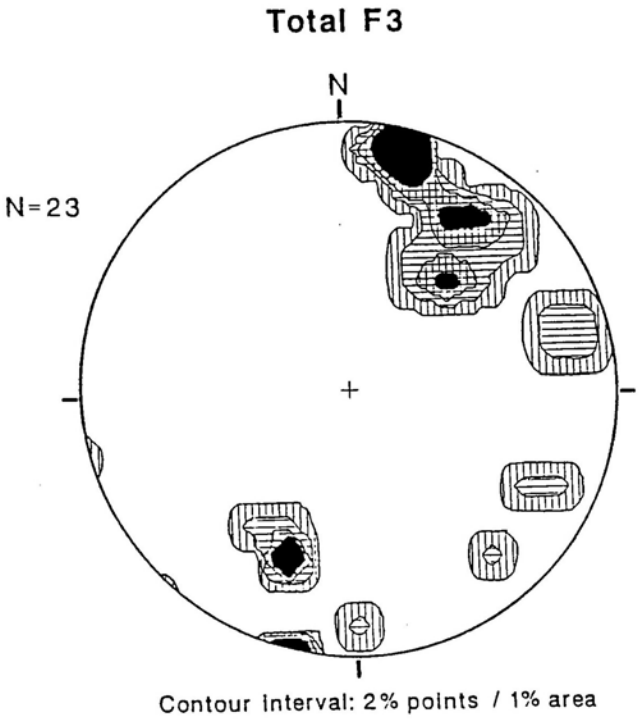

Figure 14. Contoured lower hemisphere equal area projection of mesoscopic F3 fold axes. Most have shallow, north-northeast plunges. The varied orientations of these open folds may be due to the superposition of warping on a complexly deformed preexisting fabric.

North-Striking Faults

High-angle brittle faults pervade the western part of the area and regions farther west (Figure 2; Lewis and others, 1990). Characteristics of these faults include wide zones of sericitization, brecciation, and local low-grade gold mineralization. Some vuggy quartz veins may be associated with them. The shallow apparent depth during movement suggests they postdate D2 and the intrusion of the Atlanta lobe, but the altered zones along these faults suggests that hydrothermal systems, perhaps driven by the batholith's residual heat, were still active. A $^{40}Ar/^{39}Ar$ date of 69.1 Ma on secondary muscovite from one of these faults along the west side of Newsome Creek 13 km west of Elk City (L.W. Snee, oral commun., 1991) is consistent with this interpretation. The age of faulting relative to F3 folds is unclear.

FOURTH DEFORMATION (D4)

The fourth deformation in the region produced wide-ranging effects, such as microchevron folding and retrograde metamorphism (Reid, 1959), upright shear folds with north-south trends, cataclasis with epidote growth (Greenwood, 1967), cataclastic kink folds (Morrison, 1968), and open, broad-hinged, parallel style folds with trends ranging from north to west-northwest (Wiswall and Hyndman, 1987). In this area, D4 may have been responsible for a rare, northeast-trending secondary crenulation lineation observed in micaceous metasedimentary rocks. D4 is characterized, however, by faulting along numerous northeast-striking fault zones (Figures 1 and 2). One of these, the Red Horse Creek fault, shows only minor propylitic alteration and slickenlines, but it offsets map units in an apparent left-lateral sense. Near another, the Bargamin fault along the Salmon River to the southeast of the map area (Figure 1), quartzites, granitoids, and dacite dikes are mylonitized. These mylonites contain moderately to strongly strained and sutured quartz and feldspar grains, and they show subgrain boundary development or grain-size reduction. Postmetamorphic retrogressive reactions in D4 fault zones include biotite to Fe-chlorite + K-feldspar, and sillimanite or kyanite to sericite. These features indicate low temperature, late metamorphic conditions.

The sense of motion on the D4 faults, which appears to be predominantly normal, is related to northwest-southeast Tertiary extension as indicated by dikes that parallel the faults. Similar extension directions are documented elsewhere in the region (Bennett, 1986). West of the northeast-striking Bargamin fault (Figure 1), mylonitized dacitic dikes and quartzites contain a down-dip stretching lineation in a steep northwest-dipping shear foliation. S-C mylonites developed in dikes in this zone suggest a normal down-to-the-northwest sense of movement.

FIFTH DEFORMATION (D5)

D5 is indicated not by fabrics in the rocks or a variation in their attitudes but by the apparent offset of erosional surfaces. Unconsolidated fine lacustrine to coarse fluvial Tertiary sediments are concentrated around Elk City (Figure 2) and farther west above Newsome Creek (Lewis and others, 1990). Preservation in present topographic lows bounded by some linear contacts can be explained by the downfaulting of the sediments after deposition at some higher elevation with respect to surrounding bedrock or by their original deposition in fault-bound valleys. Very coarse monolithic breccias in some places may represent colluvium from fault scarps or deep regolith that was inundated. The distribution of these breccias makes their origin due to faulting contemporaneous with deposition seem more likely. If extrusion of the Columbia River flood basalts was responsible for damming the rivers in the area, this sediment accumulation and faulting likely date from the Miocene. The orientation and locations of the faults suggest they are D3 structures that were reactivated to form grabens, e.g., east of the Newsome Creek shear zone.

METAMORPHIC ASSEMBLAGES AND P-T CONDITIONS

INTERKINEMATIC METAMORPHISM

The relative timing of D1, D2, and high-grade metamorphism is only moderately constrained. At least one interval of high-grade metamorphic crystallization was the result of an interkinematic (post-D1) metamorphic episode (Reid, 1959; Greenwood, 1967; Morrison, 1968; Standish, 1973). Static metamorphism is suggested by the scattered orientations of porphyroblasts in rocks that are only weakly overprinted by D2 structures. Peak metamorphic conditions north of the Bitterroot lobe reflect deep-seated static thermal metamorphism (Rice and others, 1988). Closer to the study area, in the Lochsa area to the northeast, sillimanite-muscovite grade metamorphism accompanied D1 deformation and was followed by an interkinematic sillimanite-grade metamorphism, as shown by statically formed sillimanite overprinting well-aligned

D1 sillimanite (Morrison, 1968). The interpretation that high-grade metamorphism was synchronous with D1 deformation in the study area (Reid, 1959; Greenwood, 1967) is equivocal because the common foliation-parallel alignment of porphyroblasts can be attributed to D2 shear.

PEAK METAMORPHIC CONDITIONS

Peak pressure and temperature conditions were estimated using the petrogenetic grid approach (Figure 15). The interkinematic metamorphic episode in the Elk City region appears to have culminated in the kyanite-muscovite and sillimanite-muscovite fields of the epidote amphibolite facies. Staurolite occurs as rare, highly altered small grains (<1 mm). The absence of this index mineral from most pelitic rocks suggests peak metamorphic temperatures in excess of 650°C-700°C (Pigage and Greenwood, 1982; Hyndman and others, 1988). Kyanite is more common (but not widespread), occurring as large (1-3 cm), euhedral, poikiloblastic, random porphyroblasts; as small (0.5-1.0 mm) euhedral matrix grains; and as rare armored relics in garnet. Sillimanite is widespread and occurs in three forms: as cloudy fibrolite, as fine-grained sillimanite needles (both in quartz and muscovite and in the matrix), and as coarser idioblastic grains commonly interleaved with biotite. Fibrolite occurs as bundles or as radiating fibrous bow-tie structures that indicate inter-kinematic crystallization (Spray, 1983).

Kyanite and sillimanite occur together in several samples. The overall stable coexistence of adjacent kyanite and sillimanite in most of these samples (Figures 3, 7, and 12) suggests peak metamorphic conditions near the kyanite-sillimanite reaction line. The paucity of staurolite, the predominance of sillimanite over kyanite, and the occurrence of fine-grained armored relics of kyanite in garnet of sillimanite-bearing pelitic rocks suggest that the paragenetic sequence is staurolite-out, kyanite-out, or sillimanite-in. Equilibrium conditions peaked in the sillimanite + muscovite (+ quartz) stability field. These relationships suggest maximum temperatures of 650°C-750°C at high pressures (8-10 Kbar; Figure 16).

Consistent with these metamorphic pressures is the average pressure of as much as 9 Kbar for the megacrystic granodiorite from the Black Hawk Mountain area (Hirt and Dragovich, 1990). This estimate is corroborated by the presence of apparently magmatic epidote in the megacrystic granodiorite, which is thought to indicate a pressure of solidification above 5 Kbar (Zen and Hammarstrom, 1984; Zen, 1985; Schmidt and Thompson, 1996).

Considerable uplift between the intrusion of the megacrystic granodiorite and the Eocene granodiorite exposed immediately south of the study area is implied by the contrast in their emplacement depths. A shallow level of the country rock during granodiorite intrusion is indicated by a narrow contact aureole around it, miarolitic cavities in related aplite dikes, and association of similar rock elsewhere with volcanic accumulations. Consistent with this field evidence is a pressure of less than 2 Kbar calculated from aluminum in hornblende (Hirt and Dragovich, 1990).

DISCUSSION

The ages of the younger deformations (D2-D5) are relatively well constrained, whereas the age of D1 is not. We will present the interpreted geologic history backwards in time to review the style, conditions, age, and possible regional significance of selected parts of D1-D5 documented in the study area. Structural evolution during D1-D4 is shown schematically in Figure 16. Estimated temporal change in depth and pressure is portrayed in Figure 17.

TIMING OF D4 AND D5

Uplift and faulting probably continue today, but the last event documented by geologic evidence occurred when north-striking faults were reactivated during Miocene (and younger?) extension. Although nowhere nearly as developed as in the Basin and Range Province, minor extension (D5) during this time seems the most likely cause of basin development and containment of the unconsolidated sediments (*Ts*, Figure 2).

The northeast orientation of the Eocene dikes in the region parallel to D4 faults and the normal motion of the faults indicated by S-C fabric in mylonite suggest that faulting and dike emplacement occurred in a northwest-southeast extensional environment. The age of the D4 fault zones is shown to be coincident with dike emplacement by mylonitization of some dacite dikes. Correlating these faults with the trans-Challis fault system to the south (Kiilsgaard and Lewis, 1985; Bennett, 1986) and the dikes with Challis-age volcanism and plutonism suggests D4 is Eocene in age.

TIMING OF D3

The north-striking faults included in the D3 phase must have had motion younger than the Atlanta lobe of the

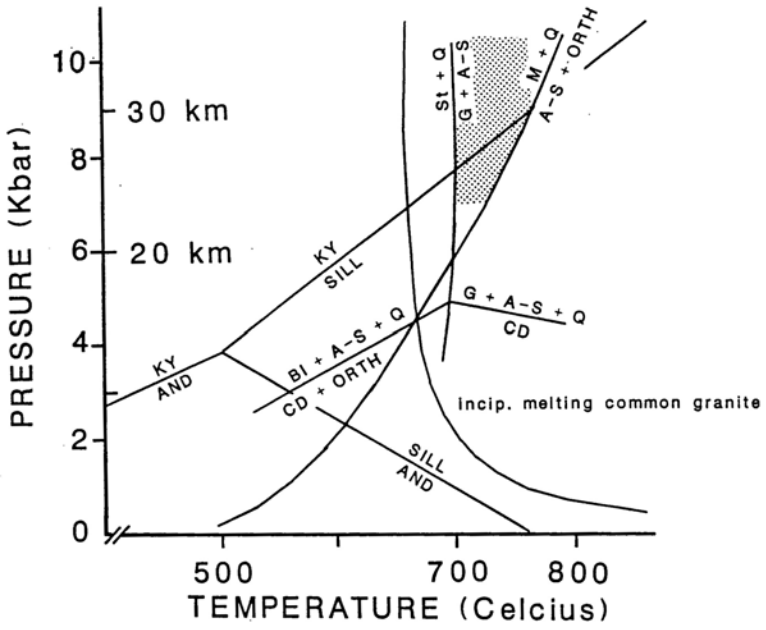

Figure 15. Petrogenetic grid containing published reaction lines for the key equilibria in the study area. The shaded region shows the peak metamorphic conditions suggested by mineral eqilibria in rocks of pelitic composition. The general absence of staurolite and exclusion of orthoclase brackets the temperature. Relatively high pressure metmorphism (8-10 Kb) is suggested by the apparent stable coexistence of kyanite and sillimanite. No aluminosilicates were observed to have crystallized or recrystallized during D2 deformation, suggesting a relaxation in metamorphic conditions. Sources of reaction are Piwinski and Wyllie (1970) for incipient melting of granite; Pigage and Greenwood (1982) for staurolite + quartz (St + Q) = garnet + aluminosilicate (G + A-S); Huang and Wyllie (1975) for muscovite + quartz (M + Q) = aluminosilicate + orthoclase (A-S + ORTH); Holdaway (1971) for kyanite (KY), sillimanite (SILL), and andalusite (AND); Hyndman and others (1988; references therein) for garnet + aluminosilicate + quartz (G + A-S + Q) = cordierite (CD), and biotite + aluminosilicate + quartz (BI + A-S + Q) = cordierite + orthoclase (CD + ORTH).

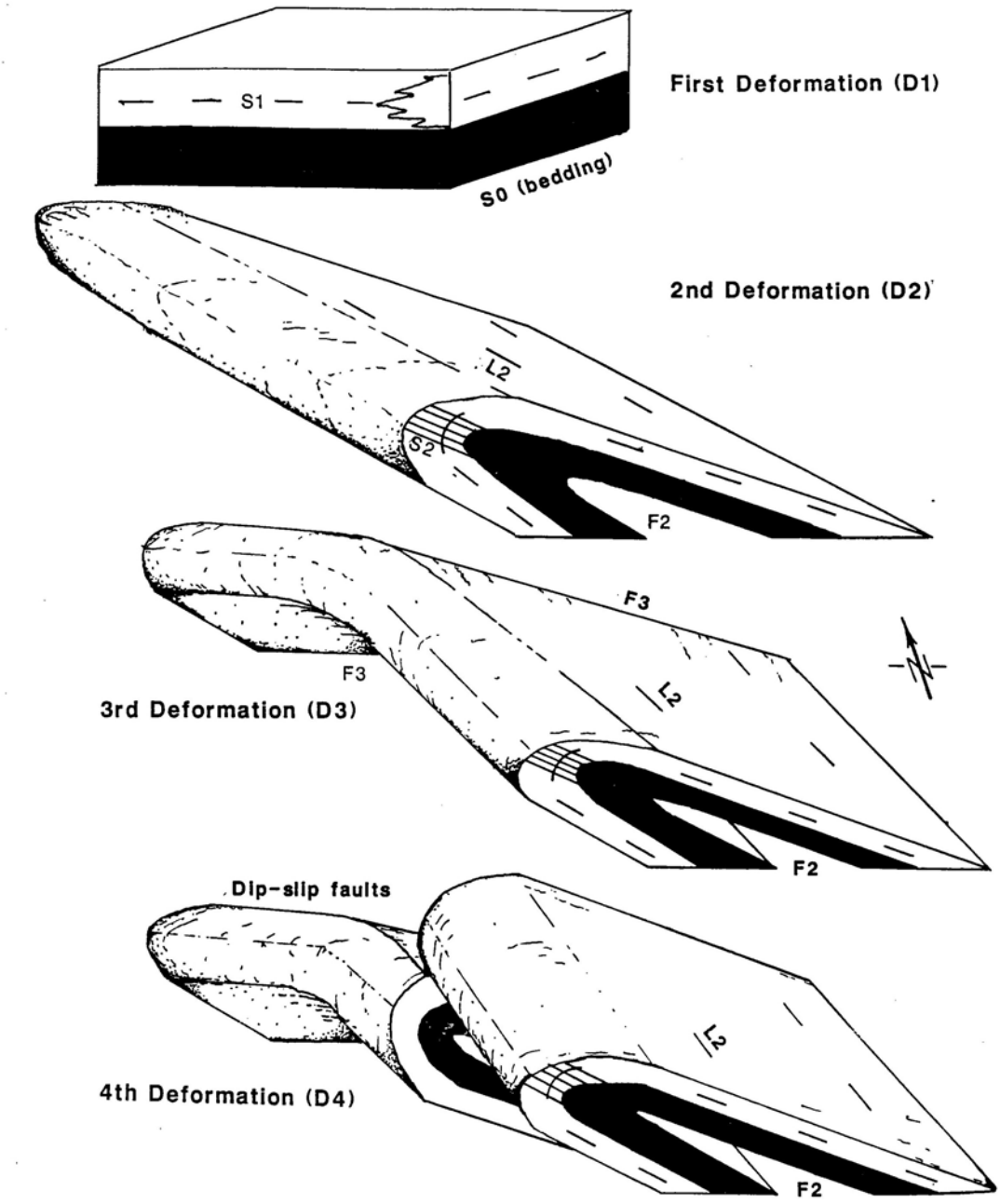

Figure 16. Schematic representation of the first through fourth deformations (D1-D4) in the Elk City region showing apparent fold and fault geometry and fabric evolution. The first deformation produced a mineral foliation, defined by biotite and muscovite, that is axial planar to rare F1 folds of the bedding. The second deformation folded the S1 foliation around northwest-southeast axes; an incipient axial planar S2 foliation developed in hinges of some F2 folds. Subhorizontal L2 mineral and crenulation lineations are parallel to the F2 fold axes. The third deformation warped the previous fabrics around a northeast-southwest axis. The fourth deformation was local warping and mylonite development along northeast-striking dip-slip faults with a minor amount of apparent left-lateral strike-slip offset.

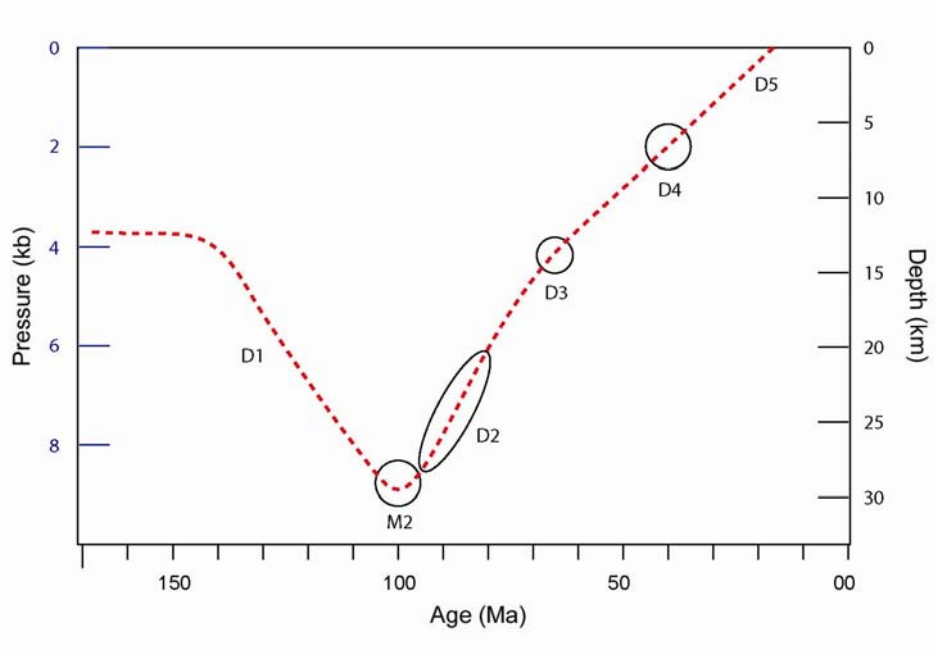

Figure 17. Change in depth and pressure of an arbitrary piece of the Elk City metamorphic sequence through deformation and metamorphism. D1 was at least tectonic thickening starting at 144 Ma with the collision of allochthonous terranes. Peak metamorphism may have been about 110 Ma or younger when rocks were at 700°C and 9 Kbar. D2 included the synkinematic intrusion of the megacrystic granodiorite (~90 Ma) at a similar depth and ended by 80 Ma when the that intrusion was about 500°C. D3 may include ~69-Ma faults that cut the Atlanta lobe and folding that is peripheral to the Coolwater culmination to the north where metamorphic ages are as young as 61 Ma (Lund and others, 2008). D4 is equated with Eocene extension when rocks were under about 2 kb pressure and cool enough to chill dikes. D5, identified with Basin and Range extension, is probably Miocene when Elk City rocks were at or near the surface.

Idaho batholith (Late Cretaceous), which some cut. The 69-Ma $^{40}Ar/^{39}Ar$ age on secondary muscovite in one of these faults (L.W. Snee, oral commun., 1991) is consistent with this. The F3 folds may be older than the faults and result from the expansion of the Paleocene Bitterroot lobe, but they cannot be as old as D2 because small-scale F3 folds affected fold L2 lineations. Comparable folds along the northwestern and western contacts of the Idaho batholith have been attributed to forceful emplacement or mushrooming during the intrusion of the main phase of the Bitterroot lobe of the batholith (Morrison, 1968; Wiswall and Hyndman, 1987), samples from which have been dated between 62 Ma and 55 Ma (Foster and Fanning, 1997; Gaschnig and others, 2007). Although D3 folds in the area possibly formed during this time, plunges of F2 and L2 increase northwestward toward the Lowell thrust. This suggests that D3 is related to processes there. If so, F3 folds are a manifestation of the same contraction that caused the Coolwater culmination of Lund and others (2008). That would date D3 between 73 Ma, the age of the youngest dated intrusion affected, and 68-60 Ma, the metamorphic age from zircons (Lund and others, 2008). D3 then may be responsible for deflecting the Green Mountain fault zone around the arc-affinity core of the Lowell thrust if it had earlier been continuous with the shear zones to the northwest. Although transverse faulting is indicated for the Green Mountain fault, it is unlikely to account for the juxtaposition of the augen gneiss-bearing rocks with Belt rocks. This is because the former are currently distributed from about 120 km southeast to 150 km northwest of Elk City.

TIMING AND SIGNIFICANCE OF D2

D2 produced greater strain at greater depth than any of the subsequent deformations. The observation that L2 pervades the megacrystic granodiorite but not all Cretaceous granitic material, e.g., some migmatites and younger phases of the Idaho batholith, suggests that D2 ended sometime between 88 Ma (the age of megacrystic rock in the Atlanta lobe; Lewis and others, 1987) and 73 Ma (the minimum age of the generally isotropic biotite granodiorite in the western part of the area; Criss and Fleck, 1987). The end of D2 probably is not younger than the 80 Ma $^{40}Ar/^{39}Ar$ hornblende cooling age of the megacrystic granodiorite (L.W. Snee, oral commun., 1991).

How much of D2 preceded the intrusion of the megacrystic granodiorite is unknown. D2 possibly included eastward thrusting on the Brushy Gulch-Red River thrust and related faults before the emplacement of the 95-90 Ma early Idaho batholith plutons, as suggested by Lund and others (2008). If so, the Green Mountain fault may have reactivated only part of the Brushy Gulch-Red River thrust, after the intrusion of the megacrystic granodiorite, and diverge from it elsewhere.

INTERKINEMATIC METAMORPHISM

For many years the Idaho batholith was thought to have caused heating of the country rocks because the regional metamorphic zones are roughly concentric around the batholith (Hietanen, 1962; Hamilton, 1963; Onasch, 1987; Myers, 1982). But the observations here of F2-folded sillimanite and aluminosilicate petrogenesis support interkinematic metamorphism before D2 and thus before the intrusion of the early phases of the batholith (93 Ma; Lund and Snee, 1988). Sillimanite also appears to predate the batholith northwest of the Bitterroot lobe (Reid and others, 1981).

We can guess at the timing of interkinematic metamorphism by appealing to a model for the thermal evolution of thickened crust (Patino Douce and others, 1990). We take the Barrovian metamorphic conditions (Figure 16) and the observation that some migmatites appear to have a synkinematic anatectic origin to indicate that the model is applicable. The model suggests that the rocks could have spent no more than a few tens of millions of years at depth before they melted. The interpretation that Cretaceous magmas in the area appear to be derived not from the mica- and amphibole-bearing mid-crustal metamorphic rock but from granulites of the lower crust may suggest that the time the micaceous rocks spent at depth was too short for them to melt extensively. Thus, interkinematic recrystallization may not have peaked before about 110 Ma with the last stage of the petrogenetic sequence, sillimanite-muscovite zone metamorphism, synchronous with the earliest tonalite phases of the Bitterroot lobe of the Idaho batholith (e.g., Rice and others, 1988). This is consistent with a Lu-Hf Cretaceous date of about 110 Ma on garnet from a calc-silicate quartzite of the Golden metamorphic sequence north of Lick Point (Art Bookstrom, oral commun., 2008).

Not all metamorphism, however, need be Cretaceous. Recent Lu-Hf geochronology of garnet-bearing rocks from near the kyanite-in isograd northwest of the area reveals ages in the range of 1.3 Ga to 1.1 Ga (Zirakparvar and others, 2006). Some rocks closer to those dated contain two visually distinct garnets (e.g., Lewis and others, 2007a) that could result from two distinct ages of growth. Thus, some garnet and kyanite there and in the Elk City area possibly date from the Mesoproterozoic.

TIMING AND STYLE OF D1

The timing and style of D1 are difficult to unravel, perhaps because more than one structural event formed the regional foliation and especially if some of the interkinematic metamorphism was Mesoproterozoic. Possibilities include the recrystallization of an original sedimentary fabric during burial at some time following deposition, and the shear during extension or thrust stacking. Crustal thickening during Cretaceous thrusting (Skipp, 1987) is a reasonable mechanism to generate D1 tectonites and would provide conditions for interkinematic high-grade metamorphism. Given the model for the origin of migmatites from partial melting in a thrust stack (Patino Douce and others, 1990), this stacking would have to be mid-Cretaceous in age, which means that it postdates the initiation of the Salmon River suture. This mid-Cretaceous timing permits a single protracted event to account for D1, high-grade metamorphism, and D2. Contraction at this time could be attributed to the docking of exotic terranes or just to the Sevier orogeny. The juxtaposition of the augen gneiss-bearing rocks with the Belt along a major intracontinental thrust could have been during D1.

It is unlikely, however, that all of "D1" was Cretaceous in age. The angular unconformity below Cambrian strata in the region attests to Precambrian folding and uplift. The deformation and metamorphism of Belt Supergroup strata to the northwest of the field area have been ascribed to multiple events (Reid and others, 1981). The apparent truncation of a fold system to the southeast in the Yellowjacket Formation near Shoup by the 1,370-Ma augen gneiss and the overprinting of a biotite-grade regional metamorphic assemblage by its contact aureole (Evans and Zartman, 1990; and references therein) document a Proterozoic history for the Shoup area that appears to include burial, compression, and then magmatism. A similar history proposed for the Elk City area, however, was based on field observations of the augen gneiss in axial zones of F1 folds, which were interpreted to indicate that the S1 foliation in the augen gneiss was developed during intrusion (Greenwood, 1967; Reid and others, 1973). This now seems unlikely because Greenwood's observations may have been of the Cretaceous megacrystic granodiorite, not the Mesoproterozoic augen gneiss, in folds which are F2 by our definitions; also, the rapakivi texture and chemical composition of the augen gneiss suggest an anorogenic origin. The approximate 1,370 Ma age of intrusion coincides with widespread anorogenic magmatism and rifting in North America (Anderson, 1983). An anorogenic origin, however, does not require that the intrusion of the augen gneiss protolith be passive. Intrusion into extensional shears could account for the sill-like geometry of the augen gneiss and some of its fabric (Hutton and others, 1990). In addition, all of these mechanisms could have inherited a fabric dating from original deposition (Norwick, 1972, 1977).

SUMMARY

The Elk City area had a long, complex, and as yet incompletely understood history that includes at least five deformations: D1, an enigmatic event in the Cretaceous(?) or Proterozoic(?), D2 in the Late Cretaceous, D3 in the Paleocene, D4 in the Eocene, and D5 in the Miocene. The last four proceeded at ever shallower levels and generally with decreasing strain during well-documented regional events. The peak of metamorphism occurred under conditions not much different from those that existed when the first phases of the Idaho batholith intruded, and likely predated the batholith by not more than a few tens of millions of years. The deep burial of the pre-batholith rock to achieve the peak metamorphic conditions most likely was tectonic, which may account for the first deformation (D1) fabrics and structures seen in outcrop. Although the antiquity of most rocks in the area permits multiple and varied mechanisms to contribute to their metamorphic and structural history, we could not isolate the postulated Cretaceous deformations sufficiently well to prove it. We were unable to duplicate Greenwood's (1967) observation of augen gneiss in the cores of F1 folds as evidence of Proterozoic deformation. This may be because we applied an apparently more restrictive definition of F1 folds, because Greenwood's observations pertain to the megacrystic granodiorite, or because we just did not find the critical exposures.

Because this work is based on only one field season and few analytical data, more research should refine some of these conclusions and resolve the origin of D1 or its parts. For instance: pegmatites in the area should be dated and their fabrics examined relative to those in surrounding rock following Reid's (1959) observation that foliated pegmatites containing biotite have a different age than those with muscovite; garnet should be dated with Lu-Hf isotopes, especially for comparison with fabrics involved and across units in the area; a better sense of postmetamorphic displacement on faults and their locations should be obtained through further study of mineral assemblages in rocks with similar chemistry.

ACKNOWLEDGMENTS

Initial analysis and documentation for this project was completed by Dragovich while employed by the Idaho Geological Survey. Special thanks are extended to the following: Western Washington University for supplying laboratory space and assistance, Paul Riley who ably mapped with the authors in the study area, Ned Brown who helped with some mineral identification and PT interpretation, Bill Hirt for the hornblende microprobe analysis, and Darrel Cowan and Rolland Reid for careful review and thoughtful suggestions of an early version of this paper. This research relied heavily on previous work by Rolland Reid and Bill Greenwood who studied extensively in the Elk City region. Little could have been accomplished without this previous geologic framework.

REFERENCES

Anderson, J.L., 1983, Proterozoic anorogenic granite plutonism of North America: Geological Society of America Memoir 161, p. 133-154.

Anderson, H.E., and D.W. Davis, 1995, U-Pb geochronology of the Moyie sills, Purcell Supergroup, southeastern British Columbia: Implications for the Mesoproterozoic geological history of the Purcell (Belt) Basin: Canadian Journal of Earth Sciences, v. 32, no. 8, p. 1180-1193.

Bennett, E.H., 1986, Relationship of the trans-Challis fault system in central Idaho to Eocene Basin and Range extension: Geology, v. 14, no. 6, p. 481-484.

Bird, P., 1998, Kinematic history of the Laramide orogeny in latitudes 35°-49° N, western United States: Tectonics, v. 17, p. 780-801.

———, 2002, Stress direction history of the western United States and Mexico since 85 Ma: Tectonics, v. 21, no. 3, p. 1-12.

Bittner, E., 1987, Migmatite zones in the Bitterroot lobe of the Idaho batholith, *in* T.L. Vallier and H.C. Brooks, eds., Geology of the Blue Mountains Regions of Oregon, Idaho and Washington: U.S. Geological Survey Professional Paper 1436, p. 73-93.

Burmester, R.F., J. Dragovich, and R.S. Lewis, 1990, Preliminary geologic map of the Red River Hot Springs-Elk City area, Idaho County, Idaho: Idaho Geological Survey Technical Report 90-3, scale 1:62,500.

Campbell, A.B., 1959, Precambrian-Cambrian unconformity in northwestern Montana and northern Idaho: Geological Society of America Bulletin, v. 70, no. 12, pt. 2, p. 1776.

Chase, R.B., 1973, Petrology of the northeastern border zone of the Idaho batholith, Bitterroot Range, Montana: Montana Bureau Mines Geology Memoir 43, 28 p.

Clark, S.H.B., 1973, Interpretation of a high grade Precambrian terrane in northern Idaho: Geological Society of America Bulletin, v. 84, p. 1999-2004.

Criss, R.E., and R.J. Fleck, 1987, Petrogenesis, geochronology and hydrothermal alteration systems of the northern Idaho batholith and adjacent areas based on $^{18}O/^{16}O$, D/H, $^{87}Sr/^{86}Sr$, K/Ar and $^{40}Ar/^{39}Ar$ studies, *in* T.L. Vallier and H.C. Brooks, eds., Geology of the Blue Mountains Regions of Oregon, Idaho and Washington: U.S. Geological Survey Professional Paper 1436, p. 95-138.

Devlin, W.J., and G.C. Bond, 1988, The initiation of the early Paleozoic Cordilleran miogeocline: Evidence from the uppermost Proterozoic-Lower Cambrian Hamill Group of southeastern British Columbia: Canadian Journal of Earth Sciences, v. 25, no. 1, p. 1-19.

Doughty, P.T., and K.R. Chamberlain, 1996, Salmon River arch revisited: New evidence for 1370 Ma rifting near the end of deposition in the Middle Proterozoic Belt basin: Canadian Journal of Earth Sciences, v. 33, p. 1037-1052.

Evans, K.V., J.N. Aleinikoff, J.D. Obradovich, and C.M. Fanning, 2000, SHRIMP U-Pb geochronology of volcanic rocks, Belt Supergroup, western Montana: Evidence for rapid deposition of sedimentary strata: Canadian Journal of Earth Sciences, v. 37, no. 9, p. 1287-1300.

Evans, K.V., and L.B. Fischer, 1986, U-Pb geochronology of two augen gneiss terranes, Idaho—New data and tectonic implications: Canadian Journal of Earth Sciences, v. 23, p. 1919-1927.

Evans, K.V., and R.E. Zartman, 1990, U-Th-Pb and Rb-Sr geochronology of middle Proterozoic granite and augen gneiss, Salmon River Mountains, east-central Idaho: Geological Society of America Bulletin, v. 102, p. 63-73.

Foster, D.A., and C.M. Fanning, 1997, Geochronology of the northern Idaho batholith and the Bitterroot metamorphic core complex: Magmatism preceding and contemporaneous with extension: Geological Society of America Bulletin, v. 109, no. 4, p. 379-394.

Gaschnig, R.M., J. Vervoort, R.S. Lewis, E. King, and J. Valley, 2007, Multiple punctuated pulses of voluminous silicic magmatism in Idaho: In situ geochronology and isotope geochemistry of the Idaho batholith:

Geological Society of America Abstracts with Programs, v. 39, no. 6, p. 608.

Greenwood, W.R., 1967, Genesis and history of the augen gneiss of Red River, Idaho County, Idaho: University of Idaho Ph.D. dissertation, 76 p.

Greenwood, W.R., and D.A. Morrison, 1973, Reconnaissance geology of the Selway-Bitterroot Wilderness Area: Idaho Bureau of Mines and Geology Pamphlet 154, 30 p.

Greenwood, W.R., and R.R. Reid, 1969, The Columbia arc: New evidence for pre-Tertiary rotation: Geological Society of America Bulletin, v. 80, p. 1797-1800.

Hamilton, W., 1963, Metamorphism in the Riggins region, western Idaho: U.S. Geological Survey Professional Paper 436, 95 p.

Harrison, T.M., 1981, Diffusion of ^{40}Ar in hornblende: Contributions to Mineralogy and Petrology, v. 78, no. 3, p. 324-331.

Harrison, T.M., I. Duncan, and I. McDougall, 1985, Diffusion of ^{40}Ar in biotite: Temperature, pressure and compositional effects: Geochimica et Cosmochimica Acta, v. 49, no. 11, p. 2461-2468.

Hietanen, A., 1962, Metasomatic metamorphism in western Clearwater County, Idaho: U.S. Geological Survey Professional Paper 344-A, p. A1-A116.

Hirt, W.H., and J.D. Dragovich, 1990, Application of a hornblende-plagioclase geothermometer to estimation of the crystallization conditions of two plutons emplaced at very different crustal levels in north-central Idaho: Geological Society of America Abstracts with Programs, v. 22, n. 7, p. 346.

Holdaway, M.J., 1971, Stability of andalusite and the aluminum silicate phase diagram: American Journal of Science, v. 271, p. 97-131.

House, M.A., S.A. Bowring, and K.V. Hodges, 2002, Implications of middle Eocene epizonal plutonism for the unroofing history of the Bitterroot metamorphic core complex, Idaho-Montana: Geological Society of America Bulletin, v. 114, no. 4, p. 448–461.

House M.A., K.V. Hodges, and S.A. Bowring, 1997, Petrological and geochronological constraints on regional metamorphism along the northern border of the Bitterroot batholith: Journal of Metamorphic Geology, v. 15, no. 6, p. 753-764.

Huang, W.L., and P.J. Wyllie, 1975, Melting reactions in the system $NaAlSi_3O_8$-$KAlSi_3O_8$-SiO_2 to 35 kilobars, dry and with excess water: Journal of Geology, v. 83, p. 737-748.

Hutton, D.H.W., T.J. Dempster, P.E. Brown, and S.D. Becker, 1990, A new mechanism of granite emplacement: Intrusion in active extensional shear zones: Nature, v. 343, p. 452-455.

Hyndman, D.W., 1989, Formation of the northern Idaho batholith and the related mylonite of the western Idaho suture zone, *in* V.E. Chamberlain, R.M. Breckenridge, and B. Bonnichsen, eds., Guidebook to the Geology of Northern and Western Idaho and Surrounding Area: Idaho Geological Survey Bulletin 28, p. 51-64.

Hyndman, D.W., D. Alt, and J.W. Sears, 1988, Post-Archean metamorphic and tectonic evolution of western Montana and northern Idaho, *in* W.G. Ernst, ed., Metamorphism and Crustal Evolution of the Western United States: Rubey Volume VII, Prentice-Hall, p. 333-361.

Kiilsgaard, T.H., and R.S. Lewis, 1985, Plutonic rocks of Cretaceous age and faults in the Atlanta lobe of the Idaho batholith, Challis quadrangle, *in* D.H. McIntyre, ed., Symposium on the Geology and Mineral Deposits of the Challis 1° x 2° Quadrangle, Idaho: U.S. Geological Survey Bulletin 1658, p. 29-42.

Leach, G.B., 1962, Metamorphism and granitic intrusion of Precambrian age in southeastern British Columbia: Geological Survey of Canada Paper 62-13, 8 p.

Lewis, R.S., R.F. Burmester, and E.H. Bennett, 1998, Metasedimentary rocks between the Bitterroot and Atlanta lobes of the of the Idaho batholith and their relationship to the Belt Supergroup, *in* R.B. Berg, ed., Belt Symposium III: Montana Bureau of Mines and Geology Special Publication 112, p. 130-144.

Lewis, R.S., R.F. Burmester, E.H. Bennett, and D.L. White, 1990, Preliminary geologic map of the Elk City region, Idaho County, Idaho: Idaho Geological Survey Technical Report 90-2, scale 1:100,000.

Lewis, R.S., R.F. Burmester, J.D. Kauffman, R.M. Breckenridge, K.L. Schmidt, M.D. McFaddan, and P.E. Myers, 2007a, Geologic map of the Kooskia 30 x 60 minute quadrangle, Idaho: Idaho Geological Survey Digital Web Map 93, scale 1:100,000.

Lewis, R.S., R.F. Burmester, M.D. McFaddan, B.A. Eversmeyer, C.A. Wallace, and E.H. Bennett, 1992a, Geologic map of the upper North Fork of the Clearwater River drainage, northern Idaho: Idaho Geologic Survey Geologic Map 20, scale 1:100,000.

Lewis, R.S., R.F. Burmester, M.D. McFaddan, J.D. Kauffman, P.T. Doughty, W.L. Oakley, and T.P. Frost, 2007b, Geologic map of the Headquarters 30 x 60 minute quadrangle, Idaho: Idaho Geological Survey Digital Web Map 92, scale 1:100,000.

Lewis, R.S., R.F. Burmester, R.W. Reynolds, E.H. Bennett, P.E. Myers, and R.R. Reid, 1992b, Geologic map of the Lochsa River area, northern Idaho: Idaho Geologic Survey Geologic Map 19, scale 1:100,000.

Lewis, R.S., J.H. Bush, R.F. Burmester, J.D. Kauffman,

D.L. Garwood, P.E. Myers, and K.L. Othberg, 2005, Geologic map of the Potlatch 30 x 60 minute quadrangle, Idaho: Idaho Geological Survey Geologic Map 41, scale 1:100,000.

Lewis, R.S., T.H. Kiilsgaard, E.H. Bennett, and W.E. Hall, 1987, Lithologic and chemical characteristics of the central and southeastern parts of the southern lobe of the Idaho batholith, *in* T.L. Vallier and H.C. Brooks, eds., Geology of the Blue Mountains Regions of Oregon, Idaho, and Washington: U.S. Geological Survey Professional Paper 1436, p. 171-196.

Lewis, R.S., J.D. Vervoort, R.F. Burmester, W.C. McClelland, and Z. Chang, 2007c, Geochronological constraints on Mesoproterozoic and Neoproterozoic(?) high-grade metasedimentary rocks of north-central Idaho, *in* P.K. Link and R.S. Lewis, eds., Proterozoic Geology of Western North America and Siberia: Society of Sedimentary Petrology (SEPM) Special Publication 86, p. 37-53.

Link, P.K., C.M. Fanning, K.V. Lund, and J.N. Aleinikoff, 2007, Detrital zircons, correlation and provenance of Mesoproterozoic Belt Supergroup and correlative strata of east-central Idaho and southwest Montana, *in* P.K. Link and R.S. Lewis, eds., Proterozoic Geology of Western North America and Siberia: Society of Sedimentary Petrology (SEPM) Special Publication 86, p. 101-128.

Lund, Karen, J.N. Aleinikoff, K.V. Evans, and C.M. Fanning, 2003, SHRIMP U-Pb geochronology of Neoproterozoic Windermere Supergroup, central Idaho: Implications for rifting of western Laurentia and synchroneity of Sturtian glacial deposits: Geological Society of America Bulletin, v. 115, p. 349-372.

Lund, Karen, J.N. Aleinikoff, K.V. Evans, and M.J. Kunk, 2004a, Proterozoic basins and orogenic belts of central Idaho: Geological Society of America Abstracts with Programs, v. 36, no. 5, p. 271.

Lund, Karen, J.N. Aleinikoff, K.V. Evans, and R.G. Tysdal, 2004b, Central Idaho thrust belt: Geological Society of America Abstracts with Programs, v. 36, no. 5, p. 545.

Lund, Karen, J.N. Aleinikoff, E.Y. Yacob, D.M. Unruh, and C.M. Fanning, 2008, Coolwater culmination: Sensitive high-resolution ion microprobe (SHRIMP) U-Pb and isotopic evidence for continental delamination in the Syringa embayment, Salmon River suture, Idaho: Tectonics, v. 27, 32 p.

Lund, Karen, and L.W. Snee, 1988, Metamorphism, structural development, and age of the continent-island arc juncture in west-central Idaho, *in* W.G. Ernst, ed., Metamorphism and Crustal Evolution of the Western United States: Rubey Volume III, Prentice Hall, p. 297-331.

Lund, Karen, L.W. Snee, and K.V. Evans, 1986, Age and genesis of precious metals deposits, Buffalo Hump district, central Idaho: Implications for depth of emplacement of quartz veins: Economic Geology, v. 81, no. 4, p. 990-996.

Mattinson, J.M., 1978, Age, origin and thermal histories of some plutonic rocks from the Salinian block of California: Contributions to Mineralogy and Petrology, v. 67, no. 3, p. 233-245.

McClelland, W.C., and J.S. Oldow, 2007, Late Cretaceous truncation of the western Idaho shear zone in the central North American Cordillera: Geology, v. 35, no. 8, p. 723–726.

McClelland, W.C., J.D. Vervoort, J.S. Oldow, A.J. Watkinson, and, G.S. Shaw, 2005, Grenville-age metamorphism on the western margin of Laurentia, northern Idaho: Evidence from Lu-Hf garnet geochronology: 15th Annual V.M. Goldschmidt Conference Abstracts, Special Supplement to Geochimica et Cosmochimica Acta, p. A305.

McDougall, I., and T.M. Harrison, 1999, Geochronology and Thermochronology by the $^{40}Ar/^{39}Ar$ Method, 2nd Edition: Oxford University Press, 269 p.

McMechan, M.E., and R.A. Price, 1982, Superimposed low-grade metamorphism in the Mount Fisher area, southeastern British Columbia: Implications for the East Kootenay orogeny: Canadian Journal of Earth Sciences, v. 19, p. 476-489.

Miller, F.K., 1994, The Windermere Group and late Proterozoic tectonics in northeastern Washington and northern Idaho, *in* Raymond Lasmanis and E.S. Cheney, eds., Regional Geology of Washington State: Washington Department of Natural Resources, Division of Geology and Earth Resources, Bulletin 80, p. 1-19.

Morrison, D.A., 1968, Reconnaissance geology of the Lochsa area, Idaho County, Idaho: University of Idaho Ph.D. dissertation, 123 p.

Myers, P.E., 1982, Geology of the Harpster area, Idaho County, Idaho: Idaho Bureau of Mines and Geology Bulletin 25, 46 p.

Norwick, S.A., 1972, The regional Precambrian metamorphic facies of the Prichard Formation of western Montana and northern Idaho: University of Montana Ph.D. dissertation, 129 p.

———, 1977, Precambrian amphibolite facies metamorphism in the Belt rocks of northern Idaho: Geological Society of America Program with Abstracts, v. 9, no. 6, p. 753.

Onasch, C.M., 1987, Temporal and spatial relations between folding, intrusion, metamorphism, and thrust

faulting in the Riggins area, west-central Idaho, *in* T.L. Vallier and H.C. Brooks, eds., Geology of the Blue Mountains Regions of Oregon, Idaho and Washington: U.S. Geological Survey Professional Paper 1436, p. 139-149.

Paterson, S.R., R.H. Vernon, and O.T. Tobish, 1989, A review of criteria for the identification of magmatic and tectonic foliations in granitoids: Journal of Structural Geology, v. 11, p. 349-363.

Patino Douce, A.E., E.D. Humphreys, and A.D. Johnston, 1990, Anatexis and metamorphism in tectonically thickened continental crust exemplified by the Sevier hinterland, western North America: Earth and Planetary Science Letters, v. 97, p. 290-315.

Payne, J.D., 2004, Kinematic and geochronological constraints for the truncation of the Salmon River suture zone: University of Idaho M.S. thesis, 43 p.

Pigage, L.C., and H.J. Greenwood, 1982, Internally consistent estimates of pressure and temperature: The staurolite problem: American Journal of Science, v. 282, p. 943-969.

Piwinski, A.J., and P.J. Wyllie, 1970, Experimental studies of igneous rock series: Felsic body suite from Needle Point pluton, Wallowa batholith, Oregon: Journal of Geology, v. 78, p. 52-76.

Reid, R.R., 1959, Reconnaissance geology of the Elk City region, Idaho: Idaho Bureau of Mines and Geology Pamphlet 120, 74 p.

———, 1987, Structural geology and petrology of a part of the Bitterroot lobe of the Idaho batholith, *in* T.L. Vallier and H.C. Brooks, eds., Geology of the Blue Mountains Regions of Oregon, Idaho and Washington: U.S. Geological Survey Professional Paper 1436, p. 37-58.

Reid, R.R., W.R. Greenwood, and D.A. Morrison, 1970, Precambrian metamorphism of the Belt Supergroup in Idaho: Geological Society of America Bulletin, v. 81, no. 3, p. 915-918.

Reid, R.R., W.R. Greenwood, and G.L. Nord, Jr., 1981, Metamorphic petrology and structure of the St. Joe area, Idaho: Geological Society of America Bulletin, Part II, v. 92, p. 94-205.

Reid, R.R., D.A. Morrison, and W.R. Greenwood, 1973, The Clearwater orogenic zone: A relict of Proterozoic orogeny in central and northern Idaho, *in* Belt Symposium 1973, Volume I: Idaho Bureau of Mines and Geology, p. 10-56.

Rice, J.M., T.W. Grover, and H.M. Lang, 1988, P-T evolution of the St. Joe-Clearwater region, northern Idaho: Geological Society of America Abstracts with Programs, v. 20, no. 7, p. A18.

Russell, C.W., and J. Gabites, 2005, Elevated $^{87}Sr/^{86}Sr$ ratios from mafic intrusions in the Atlanta lobe of the Idaho batholith: Idaho Geological Survey Technical Report 05-1, 61 p.

Ryan, B.D., and J. Blenkinsop, 1971, Geology and geochronology of the Hellroaring Creek stock, British Columbia: Canadian Journal of Earth Sciences, v. 8, p. 85-95.

Schmidt, M.W., and A.B. Thompson, 1996, Epidote in calc-alkaline magmas: An experimental study of stability, phase relationships, and the role of epidote in magmatic evolution: American Mineralogist, v. 81, p. 462-474.

Sears, J.W., K.R. Chamberlain, and S.N. Buckley, 1998, Structural and U-Pb geochronological evidence for 1.47 Ga rifting in the Belt basin, western Montana: Canadian Journal of Earth Sciences, v. 35, p. 467-475.

Selverstone, J., B. Wernicke, and E.A. Aliberti, 1992, Intracontinental subduction and hinged unroofing along the Salmon River suture zone, west central Idaho: Tectonics, v. 11, p. 124-144.

Sha, G.S., 2004, The tectonic evolution of the Boehls Butte-Clearwater core complex, north-central Idaho: Washington State University M.S. thesis, 143 p.

Sha, G.S., J.D. Vervoort, A.J. Watkinson, P.T. Doughty, Julie Prytulak, R.G. Lee, and P.B. Larson, 2004, Geochronologic constraints on the tectonic evolution of the Boehls Butte-Clearwater core complex: Evidence from 1.01 Ga garnets: Geological Society of America Abstracts with Programs, v. 36, no. 4, p. 72.

Shenon, P.J., and J.C. Reed, 1934, Geology and ore deposits of the Elk City, Orogrande, Buffalo Hump, and Tenmile districts, Idaho County, Idaho: U.S. Geological Survey Circular 9, 89 p.

Simpson, C., and S.M. Schmid, 1983, An evaluation of criteria to deduce the sense of movement in sheared rocks: Geological Society of America Bulletin, v. 94, p. 1281-1288.

Skipp, Betty, 1987, Basement thrust sheets in the Clearwater orogenic zone, central Idaho and western Montana: Geology, v. 15, no. 3, p. 220-224.

Spry, Alan, 1969, Metamorphic Textures (2nd printing 1986): Pergamon Press, 352 p.

Standish, R.P., 1973, Structural geology and metamorphism of the Mallard-Larkins Peak area, Clearwater and Shoshone counties, Idaho: University of Idaho M.S. thesis, 82 p.

Stewart, J.H., 1972, Initial deposits in the Cordilleran geosyncline: Evidence of a Late Precambrian (<850 m.y.) continental separation: Geological Society of America Bulletin, v. 83, p. 1345-1360.

Tysdal, R.G., 2000, Revision of Middle Proterozoic

Yellowjacket Formation, central Idaho: U.S. Geological Survey Professional Paper 1601–A, p. A1-A13.

Vernon, R.H., V.A. Williams, and W.F. D'Arcy, 1983, Grainsize reduction and foliation development in a deformed granitoid batholith: Tectonophysics, v. 92., p. 123-145.

Vervoort, J.D., W.C. McClelland, J.S. Oldow, A.J. Watkinson, and G.S. Sha, 2005, Grenville-age metamorphism on the western margin of Laurentia, northern Idaho: Evidence from Lu-Hf garnet geochronology: Geological Society of America Abstracts with Programs, v. 37, no. 7, p. 89.

Winston, Don, P.K. Link, and Nate Hathaway, 1999, The Yellowjacket is not the Prichard and other heresies: Belt Supergroup correlations, structure and paleogeography, east-central Idaho, *in* S.S. Hughes and G.D. Thackray, eds., Guidebook to the Geology of Eastern Idaho: Idaho Museum of Natural History, p. 3-20.

Wiswall, C.G., 1979, Structure and petrography below the Bitterroot dome, Idaho batholith, near Paradise, Idaho: University of Montana Ph.D. dissertation, 129 p.

Wiswall, C.G., and D.W. Hyndman, 1987, Emplacement of the main plutons of the Bitterroot lobe of the Idaho batholith, *in* T.L. Vallier and H.C. Brooks, eds., Geology of the Blue Mountains Regions of Oregon, Idaho and Washington: U.S. Geological Survey Professional Paper 1436, p. 59-72.

Zen, E., 1985, Implications of magmatic epidote-bearing plutons on crustal evolution in the accreted terranes of northwestern North America: Geology, v. 13, p. 266-269.

———, 1988, Tectonic significance of high-pressure plutonic rocks in the western cordillera of North America, *in* W.G. Ernst, ed., Metamorphism and Crustal Evolution of the Western United States: Rubey Volume VII, Prentice Hall, p. 41-67.

Zen, E-an, and Jane Hammarstrom, 1984, Magmatic epidote and its petrologic significance: Geology, v. 12, p. 515-518.

Zirakparvar, N.A., J.D. Vervoort, A.J. Watkinson, and J.G. Evans, 2006, TI: Lu-Hf geochronology of garnet tectonites from the northern U.S Cordillera: Evidence for protracted history of deformation and metamorphism beginning in the Late Mesoproterozoic: Eos Transactions, American Geophysical Union, v. 87, no. 52, fall meeting supplement, Abstract T31C-0461.